Advanced Materials

Biodegradable Spheres Protect Traumatically Injured Spinal Cord by Alleviating the Glutamate-Induced Excitotoxicity

--Manuscript Draft--

Manuscript Number:	adma.201706032R1
Full Title:	Biodegradable Spheres Protect Traumatically Injured Spinal Cord by Alleviating the Glutamate-Induced Excitotoxicity
Article Type:	Communication
Section/Category:	
Keywords:	acetalated dextran; spinal cord injury; alleviated excitotoxicity; glutamate adsorption; calcium ion scavenging
Corresponding Author:	Jin Fan Jiangsu Province Hospital and Nanjing Medical University First Affiliated Hospital CHINA
Additional Information:	
Question	**Response**
Please submit a plain text version of your cover letter here. **If you are submitting a revision of your manuscript, please do not overwrite your original cover letter. There is an opportunity for you to provide your responses to the reviewers later; please do not add them here**.	Dr. Jos Lenders Editor Advanced Materials Dear Dr. Jos Lenders, I am submitting the revised manuscript (adma.201706032) entitled “Biodegradable Spheres Protect Traumatically Injured Spinal Cord by Alleviating the Glutamate-Induced Excitotoxicity” by Dongfei Liu, Jian Chen, Tao Jiang, Wei Li, Yao Huang, Xiyi Lu, Zehua Liu, Weixia Zhang, Zheng Zhou, Qirui Ding, Hélder A. Santos, Guoyong Yin, Jin Fan to be published as a communication in Advanced Materials. We would like first to thank the reviewer for the constructive comments and the given possibility to reply to those comments towards the improvement of the manuscript. All the related comments raised by the reviewers have been addressed. For this, we have also conducted additional experiments, as suggested by the reviewers. Please find enclosed the point-by-point response to the reviewers’ comments, which also describe the changes made in the main text and supporting information. The marked copy of the revised manuscript shows all the changes made on revised manuscript clearly highlighted in yellow. I strongly believe that the changes introduced in the text have further improved the manuscript and the revised manuscript is now acceptable for publication. If further modifications are needed, we would be pleased to promptly make them. Thank you in advanced for your consideration! Yours Sincerely, Prof. Dr. Jin Fan Department of Orthopaedics The First Affiliated Hospital of Nanjing Medical University No. 300 Guangzhou Road, 201129 Nanjing Tel.: +358 9 2941 59661 @ email: fanjin@njmu.edu.cn Dr. Jos Lenders Editor

	Advanced Materials Dear Dr. Jos Lenders, I would like to ask for the reconsideration of the manuscript (MS No. adma.201606636) newly entitled “Biodegradable Spheres Protect Traumatically Injured Spinal Cord by Alleviating the Glutamate-Induced Excitotoxicity” by Dongfei Liu, Jian Chen, Tao Jiang, Wei Li, Yao Huang, Xiyi Lu, Zehua Liu, Weixia Zhang, Zheng Zhou, Qirui Ding, Hélder A. Santos, Guoyong Yin, Jin Fan to be published as a communication in Advanced Materials. I would like to thank you for considering our manuscript for review. I also want to thank the reviewers for the time spent and the valuable comments toward the improvement of the manuscript. The insightful commentaries undoubtedly help us to improve the overall quality of the manuscript. The revised version and point-by-point reply to the reviewers’ comments are appended to this letter. Reviewer #2 has suggested the more control groups to be added, which we strongly believe are not necessary in this manuscript and they will not change the conclusions of the current paper. Our arguments are presented below. We cannot find proper positive therapy control, because the mechanism of therapy of injured spinal cord by acetalated dextran is new. Our study demonstrates that the intrathecal administration of bare acetalated dextran microspheres can protect neurons from glutamate-induced excitotoxicity, and therefore, inhibit the second injury to the spinal cord. The neuroprotective feature of acetalated dextran microspheres is achieved by sequestering glutamate and calcium ions in CSF, reducing the calcium ions influx into neurons and inhibiting the formation of reactive oxygen species. Consequently, AcDX microspheres attenuate the expression of pro-apoptotic proteins (Calpain and Bax) and enhance the expression of anti-apoptotic protein (Bcl-2) both in vitro and in vivo. Overall, the neuroprotection effect of acetalated dextran is because of its ability to scavenge glutamate and calcium ions in cerebrospinal fluid. To the best of our knowledge, this is the first biomaterial has been proved to enhance the recovery of injured spinal cord by simple physical adsorption. We have not yet seen any other similar studies. It is impossible to add a third group with the same mechanism for spinal cord injury. Many studies on the therapy of injured spinal cord only have 2 groups: the vehicle group and the treatment group (Science 2015, 348:347-352; Science 2011, 331:928-931; Nat Nanotechnol 2014, 9:1054-1062; ACS Nano 2015, 9:1492–1505; Biomaterials 2017, 123: 63-76). This two-group setting is also because of the lack of gold standard therapeutic strategy with the same mechanism for the therapy spinal cord injury. To minimize the time consuming and expensive animal studies, as well as application of the animal 3Rs (Replacement, Reduction and Refinement) rule, we just selected the two groups for this study. We strongly believe that all the comments to this manuscript raised by the reviewer has been addressed. This manuscript is suitable for publishing in Advanced Materials. Therefore, we would like to ask for reconsideration of our revised manuscript (MS No. adma.201606636). Yours Sincerely, Prof. Dr. Jin Fan Department of Orthopaedics The First Affiliated Hospital of Nanjing Medical University No. 300 Guangzhou Road, 201129 Nanjing Tel.: +358 9 2941 59661 @ email: fanjin@njmu.edu.cn
Do you or any of your co-authors have a conflict of interest to declare?	No. The authors declare no conflict of interest.
Corresponding Author Secondary Information:	

Corresponding Author's Institution:	Jiangsu Province Hospital and Nanjing Medical University First Affiliated Hospital
Corresponding Author's Secondary Institution:	
First Author:	Dongfei Liu
First Author Secondary Information:	
Order of Authors:	Dongfei Liu
	Jian Chen
	Tao Jiang
	Wei Li
	Yao Huang
	Xiyi Lu
	Zehua Liu
	Weixia Zhang
	Zheng Zhou
	Qirui Ding
	Hélder A Santos
	Guoyong Yin
	Jin Fan
Order of Authors Secondary Information:	
Abstract:	Our study demonstrates that the intrathecal administration of bare acetalated dextran (AcDX) microspheres can protect neurons from glutamate (GLU)-induced excitotoxicity, and therefore, repair the injured spinal cord. The neuroprotective feature of AcDX microspheres is achieved by sequestering GLU and calcium ions in cerebrospinal fluid (CSF), reducing the calcium ions influx into neurons and inhibiting the formation of ROS. Consequently, AcDX microspheres attenuate the expression of pro-apoptotic proteins (Calpain and Bax) and enhance the expression of anti-apoptotic protein (Bcl-2) both in vitro and in vivo. The intrathecal administration of AcDX microspheres immediately after traumatic injury leads to histological protection in spinal tissue and functional recovery in live animals. In summary, our work opens an exciting perspective toward the application of neuroprotective AcDX for the treatment of severe neurological diseases.

Submitted to ADVANCED MATERIALS

DOI: 10.1002/adma.(please add manuscript number)

Biodegradable Spheres Protect Traumatically Injured Spinal Cord by Alleviating the Glutamate-Induced Excitotoxicity

By Dongfei Liu, Jian Chen, Tao Jiang, Wei Li, Yao Huang, Xiyi Lu, Zehua Liu, Weixia Zhang, Zheng Zhou, Qirui Ding, Hélder A. Santos*, Guoyong Yin*, Jin Fan*

Dr. D. Liu, Dr. W. Li, Z. Liu and Prof. H. A. Santos
Division of Pharmaceutical Chemistry and Technology
Faculty of Pharmacy, University of Helsinki
FI-00014, Helsinki, Finland.
Email: helder.santos@helsinki.fi (H. A. Santos)

Dr. D. Liu and Prof. H. A. Santos
Helsinki Institute of Life Science
HiLIFE, University of Helsinki
FI-0014 Helsinki, Finland

Dr. D. Liu and Dr. W. Zhang
John A. Paulson School of Applied Science and Engineering
Harvard University
MA 02138, Cambridge, USA.

J. Chen, T. Jiang, Y. Huang, Z. Zhou, Q. Ding, Prof. G. Yin and Prof. J. Fan
Department of Orthopaedics
The First Affiliated Hospital of Nanjing Medical University
Nanjing 210029, China
Email: guoyong_yin@sina.com (G. Yin) and fanjin@njmu.edu.cn (J. Fan)

T. Jiang
Department of Orthopaedics

Wuxi People's Hospital Affiliated to Nanjing Medical University
Wuxi 214023, China

X. Lu
Department of Oncology
The First Affiliated Hospital of Nanjing Medical University
Nanjing 210029, China.

Keywords: acetalated dextran; spinal cord injury; alleviated excitotoxicity; glutamate adsorption; calcium ion scavenging

Spinal cord injury (SCI) is the result of an initial mechanical disruption in the spinal cord structures (primary insult), followed by a secondary event that collectively injures the intact neighboring tissue.[1] Worldwide, an estimated 2.5 million people are living with SCI, with more than 130 thousand new injuries reported annually.[2] Traumatic SCI is a debilitating injury that have a life-long impact on the injured person. The economic cost of SCI is estimated to be approximately 9.7 billion dollars annually in the United States.[3] Despite its significant societal and economic impacts, few clinical treatments exist for traumatic SCI, and they only have limited therapeutic efficacy.[4] Therefore, new therapeutic strategies with improved therapeutic efficacy have been actively pursued.[5]

One of the promising approaches to treat traumatic SCI is using biomaterials. Several biodegradable polymers have been illustrated to support or promote axon regeneration in central nervous system. For example, the local administration of hydrogel composing of poloxamers (nonionic amphiphilic triblock copolymers) has been shown to slightly improve the functional motor recovery of injured spinal cord.[6] The self-assembled poly(ethylene glycol)−poly(D,L-lactic acid) block copolymer micelles repair the injured axonal membranes and reduce the calcium influx into axons, resulting in an improvement of locomotor function after traumatic SCI in adult rats.[7] Functional restoration of injured spinal cord has also been observed through the intravenously administration of ferulic acid modified glycol chitosan nanoparticles at 2 h post-injury.[8] Moreover, poly(lactic-co-glycolic acid),[9] poly(caprolactone fumarate)[10] and oligo[(polyethylene glycol) fumarate][11] have previously been shown to benefit the neuron repair.[12]

Recently, a biodegradable water-insoluble polymer ‘acetalated-dextran’ (AcDX) was synthesized by modifying hydroxyl groups of water-soluble dextran with 2-methoxypropene.[13] Because of its high solubility in organic solvents, AcDX and its derivatives have been formulated into micro- and nano-particles for biomedical applications, such as immunotherapy[14] and myocardial infarction treatment.[15] The immunogenicity of subunit vaccines could be enhanced by encapsulating a protein antigen and/or adjuvant within AcDX microspheres.[14] AcDX microspheres loaded with an engineered

hepatocyte growth factor fragment were employed for the treatment of myocardial infarction.[15] The cardioprotective efficacy of payload was optimal when delivered over 3 days post-intramyocardial injection, yielding the largest arterioles and the fewest apoptotic cardiomyocytes bordering the infarct.[15a]

After SCI, glutamate (GLU) floods out of injured spinal neurons, axons, and astrocytes, overexciting neighboring neurons.[16] The overexcited cells let in waves of calcium ions, which can trigger a series of destructive events, including production of highly reactive free radicals. These radicals can attack membranes and other cell organelles, and result in the neuronal death. These processes inevitably aggravate the injury of spinal cord. Hence, capturing GLU at the acute phase of injury may offer new treatment modalities for SCI therapy. In this study, we found out that the polymer AcDX itself can protect the injured spinal cord by reducing the level of GLU in cerebrospinal fluid (CSF) within hours after injection, and therefore, inhibit the GLU-induced excitotoxicity. Specifically, the intrathecally injected AcDX microspheres reduced the traumatic lesion volume, inhibited inflammatory response, protected the spinal cord neurons, and ultimately showed the improved locomotor function following traumatic SCI.

The synthesis approach of AcDX is shown in **Figure 1a**.[13] In the presence of an acid catalyst (*p*-toluenesulfonate), the modification of vicinal diols with 2-methoxypropene efficiently transformed the water soluble dextran into water insoluble AcDX.[14] Based on the ^{1}H nuclear magnetic resonance (NMR; **Figure 1b**) spectrum of AcDX, the calculated conjugation ratio was approximately 80.4%, corresponding to 48 out of 60 glucose units in a dextran (MW 10,000 g/mol) modified by 2-methoxypropene. Fourier transform infrared (FTIR; **Figure 1c**) spectra showed a clear intensity decrease of the O-H stretch at 3325 cm^{-1}, which can be ascribed to the reaction of vicinal diols with 2-methoxypropene.

Microfluidic technology provides an easy-to-use approach for the preparation of monodisperse droplets.[17] The obtained AcDX were formulated into microspheres using a microfluidic flow-

focusing device (**Figure 1d**).[18] The device was composed of two types of capillaries for which the outer diameter (about 1.0 mm) of the cylindrical tapered capillary fitted the inner dimension (about 1.1 mm) of the outer capillary. The inner oil fluid was an AcDX ethyl acetate solution (20 mg/mL) and the outer aqueous fluid contained amphiphilic Poloxamer 407 (10 mg/mL). The oil and aqueous fluids were simultaneously pumped into the microfluidic device in the opposite directions. This flow-focusing geometry forced the inner oil fluid to breakdown, forming single O/W emulsion drops at the orifice of the inner capillary. All the collected droplets were solidified through the diffusion of ethyl acetate to the external aqueous phase. As shown in the scanning electron microscope (SEM) image (**Figure 1e-i**), the obtained AcDX microspheres are all spherical. Toward the fluorescein isothiocyanate (FITC)-loaded AcDX microspheres, the fluorescence intensity distribution within microspheres was uniform (**Figure 1e-ii**), indicating a solid structure of the obtained microspheres.[19] We can see from **Figure 1e-iii**, the average particle size of AcDX microspheres was approximately 7.2 μm with a narrow size distribution (polydispersity index = 11.1%, defined as the ratio between the standard deviation and the mean diameter of particles multiplied by 100%).

To monitor the degradation behavior of AcDX microspheres, the FITC-labelled AcDX was synthesized by modifying the vicinal diols of FITC-labelled dextran with 2-methoxypropene. At pH 7.4, AcDX decomposed slowly through hydrolyzation of the acetals, regenerating the water-soluble FITC-dextran over a period of 50 days (**Figure 1f**).[15b] This degradation of AcDX microspheres is further reflected in the release profile of a model payload, FITC (**Figure 1f**). The release of FITC from AcDX microspheres was faster than that of FITC-dextran, which was only observed after 8 days of incubation. These two release profiles suggest that the payload only diffused out when the microspheres degraded, as opposed to passive diffusion through the intact microspheres. To corroborate these results, the degradation of AcDX microspheres was visualized using SEM. The morphology of the AcDX microspheres at day 1, 7, and 28 is shown in **Figure 1g**. The increased surface roughness is clearly visible for AcDX microspheres at day 1 and 7. After 1 month of incubation

at pH 7.4, most of the polymer matrix for AcDX microspheres was degraded. These SEM images correlate well with the observed FITC and FITC-dextran release profiles.

We evaluated the cytocompatibility (activity of dehydrogenases) of AcDX microspheres with primary neurons (**Figure 1h**). No obvious cytotoxicity was observed for AcDX microspheres within the tested concentration range (0.1−4.0 mg/mL) and the selected incubation time (6−96 h). Interestingly, enhanced neuron activity was observed after incubating with AcDX microspheres for 24, 48 and 72 h. After 24 h incubation, notable neuron viability enhancement was only observed for the highest concentration of AcDX microspheres (4.0 mg/mL). When the incubation time was extended to 48 h, remarkable cell viability increase was observed for AcDX microspheres with a concentration as low as 0.2 mg/mL. The cell viability enhancement effect for AcDX microspheres disappeared after increasing the incubation time to 96 h, which could be ascribed to the accumulation of by-products of cellular metabolism inside the medium. The cytocompatibility test suggests the neuroprotective effect of AcDX microspheres, especially within the concentration range of 0.2−4.0 mg/mL.

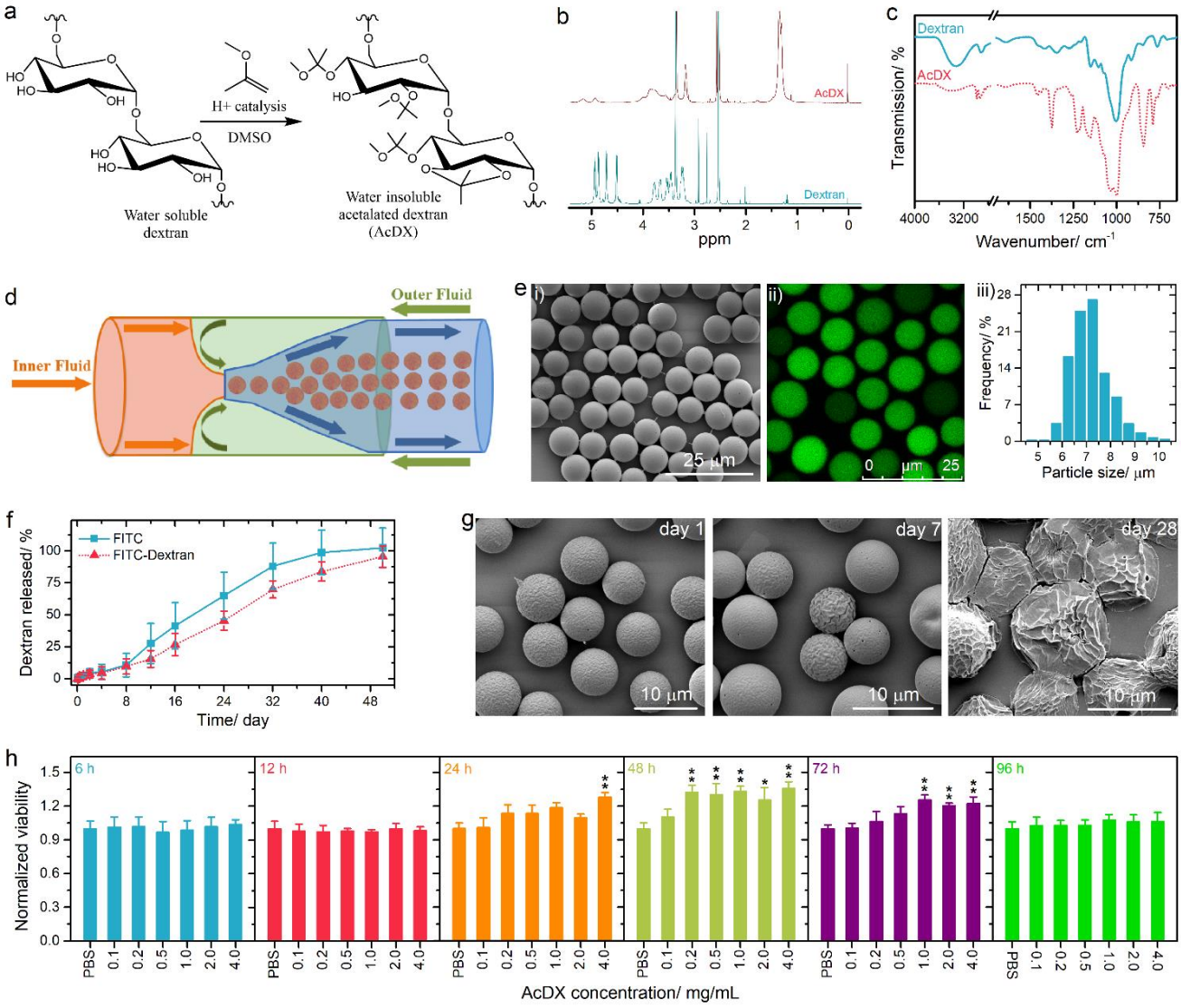

Figure 1. Preparation and characterization of AcDX microspheres and their neuronal compatibility. (**a-c**) Single-step synthesis of AcDX (a), and its NMR (b) and FTIR (c) spectra. (**d**) A schematic diagram of AcDX microspheres prepared by droplet microfluidics. (**e**) SEM (i) and confocal fluorescence microscopy (ii) images of the obtained AcDX microspheres, and their size distribution (iii). (**f**) Dissolution of FITC-dextran and FITC from AcDX microspheres in 1 × phosphate-buffered saline (1 × PBS, pH 7.4) at 37 °C (n = 3). (**g**) SEM images of AcDX microspheres after 1, 7 and 28 days of incubation in PBS (pH 7.4) at 37 °C. (**h**) The effect of AcDX microspheres (0.1-4.0 mg/mL) on the viability of primary neurons (n = 5). The neuronal viabilities incubated with AcDX

microspheres were compared with that of the PBS group. Data present as mean ± s.d.; the levels of significance were set at probabilities of $^{*}P < 0.05$ and $^{**}P < 0.01$.

To verify the neuroprotective effect of AcDX microspheres, we performed a functional motor assessment and histological injury study in Sprague-Dawley rats undergoing a weight-drop injury of the thoracic spinal cord (T10; **Figure 2**a). Regarding all the *in vivo* test, AcDX microspheres (60 μg/μL, 10 μL in total) were intrathecally administrated within 5 min post-injury. Because the cerebrospinal fluid volume in rat brain is approximately 580 μL,[20] the theoretical total volume would be approximately 590 μL after the administration of AcDX microspheres. Therefore, the final AcDX concentration (600 μg in 590 μL) achieved about 1 mg/mL, which was proved to be effective in neuron viability enhancement (**Figure 1h**). The vehicle PBS served as the control (SCI group). The degradation rate of AcDX is primarily controlled by the pH value of the incubation medium.[21] After intrathecally administration, the AcDX microspheres were dispersed in CSF. In general, CSF is clear, colorless, nearly acellular, and has a low protein concentration.[22] Since the component, especially the pH value, of CSF is similar to the *in vitro* incubation medium, the *in vivo* degradation rate of AcDX is also expected to be close to that observed *in vitro*. Instead of breaking into smaller pieces, AcDX microspheres presented an "outside-in" pattern of degradation (**Figure 1**g). Their degradation pattern indicates that AcDX microspheres would remain inside the CSF before complete degradation.

After traumatic SCI, the motor behavior was assessed by the 21-point Basso, Beattie, and Bresnahan (BBB) locomotor rating scale in open-field (**Figure 2b**). The complete hindlimb paralysis (BBB score = 0) was observed for both SCI and AcDX groups at day 1 post-injury. At day 7 post-injury, the AcDX group showed extensive movement of two joints (BBB score = 3.0 ± 0.8), which is significantly (P = 0.040) higher than the locomotor performance of SCI group (BBB score = 1.8 ± 0.5) with the extensive movement of only one joint. This superiority on the locomotor function for the AcDX group

maintained over the remainder of the motor assessment study. At day 28 post-injury, the plantar support of the paw with weight bearing only in the support stage was observed for the AcDX group with a score of 8.5 ± 1.3 on the BBB scale, whereas non-treated rats were approximately 2 points lower ($P < 0.05$). Overall, AcDX significantly improved the recovery of hindlimb motor function. In terms of the BBB score for the SCI group, it increased from 0 at day 1 post-injury to 6.5 ± 0.6 at day 28 after SCI, indicating a certain degree of spontaneous motor function recovery. This spontaneous locomotor function recovery was also included in the result of the AcDX group.

As shown by the gross morphology of the injured spinal cords, the traumatic lesion area (brown colored region) on the spinal cord was visible (**Figure 2c**). After treatment with AcDX microspheres, the lesion area was notably smaller than that of the SCI only group. A prominent pathological feature of SCI is the development of a fluid-filled cystic cavity that is bordered by reactive astrocytes.[23] The traumatic lesion cavity was identified by loss of cells using Nissl staining to study whether AcDX microspheres could reduce the lesion volume. Four weeks after injury, dramatic tissue loss on the injured spinal cord was observed (**Figure 2c**). The administration of AcDX microspheres caused a reduction in post-traumatic spinal cord tissue loss. Lesion volume was assessed by the Nissl-stained spinal cord sections, which sampled serially in the longitudinal plane with an interval of about 200 μm for each layer. As demonstrated in **Figure 2**c, the administration of AcDX microspheres significantly decreased ($P = 0.002$) the lesion volume (2.9 ± 0.9 mm^3) compared to the SCI control group (8.6 ± 1.1 mm^3).

To further understand the anatomical basis of the observed locomotor recovery, we examined the density or status of astrocytes, microglia, neurons, and axons. These cells play crucial roles in the spinal cord damage and repair. The cellular hypertrophy and increases in glial fibrillary acidic protein (GFAP) are hallmarks of astrocyte reactivity after SCI.[24] The injured spinal cord is also featured with enhanced numbers of activated Cluster of Differentiation 68 (CD68)-immunoreactive microglia.[25]

The reactive astrocytes and microglia were visualized using GFAP and CD68 immunofluorescence antibodies, respectively.

Regarding the non-treatment (SCI) group, the region in proximity to the lesion area was characterized by hypertrophic astrocytes with multiple $GFAP^+$ processes for both day 1 (**Figures 2d** and **2f**) and 28 (**Figures S1** and **S2**) post-injury, matching the appearance of SCI-associated local astrogliosis.[26] The GFAP immunoreactivity near the injury site was higher than that located further (> 10 mm) from the traumatic lesion area (**Figure 2h**). Specifically, we observed 29.4 ± 9.9% and 36.0 ± 17.8% GFAP intensity increase at 1 and 28 days post-injury, respectively, adjacent to the lesion area for SCI group. In the AcDX group, peritraumatic astrocytes were morphologically indistinguishable from astrocytes located distal to the injury site for both day 1 (**Figures 2e** and **g**) and 28 (**Figure S3** and **S4**) post-injury. At day 1 post-injury, the GFAP intensity of peritraumatic astrocytes was 15.0 ± 2.7% higher than that located further from the traumatic lesion area. This effect was continuous, because the peritraumatic GFAP intensity was only 8.1 ± 6.7% higher than that located further from the traumatic lesion area at day 28 post-injury. Hence, AcDX treatment significantly ($P < 0.05$, for both day 1 and 28 post-injury) and persistently inhibited the astrocytic response, as well as reduced the severity of initial reactive gliosis after SCI.

To evaluate the effect of AcDX treatment on microglial activation following SCI, we also quantified the number of activated microglial cells adjacent to the injury site and in the traumatic lesion area by immunodetection of $CD68^+$ microglia (**Figures 2d**, **2e**, **S1** and **S3**). At both day 1 and 28 post-injury, we did not observe any notable difference (**Figure S5**) on the number of $CD68^+$ cells in the peritraumatic area between the SCI only and AcDX groups. In contrast, a significant reduction in the number of $CD68^+$ microglia in the traumatic lesion area was observed with AcDX treatment compared to rats injected with only PBS at both day 1 ($P = 0.004$) and 28 ($P < 0.001$) post-injury (**Figure 2i**). In the lesion area, the density of microglia was 931 ± 75 per square millimeter at day 1 post-injury. After extending the time to 28 days after injury, the density of $CD68^+$ microglia increased to 2421 ± 234 per

square millimeter. Regarding the AcDX group, the $CD68^+$ microglia density only slightly increased from 727 ± 51 to 840 ± 219 per square millimeter within 28 days. At day 28 post-injury, a reduction in the number of $CD68^+$ microglia by about 65% in the traumatic lesion area was observed with AcDX treatment ($P < 0.001$) compared to rats injected with only PBS. Besides astrocytic response inhibition, AcDX efficiently restrained the inflammatory response associated to the microglia activation.[27]

Neurofilaments are cell type specific proteins in central nerve system, and qualified as potential surrogate markers of damage to neuron and axon.[28] The immunostaining analysis of 200 kDa subunit of neurofilament (NF200), which contributes to anomalous electrophoretic mobility, has been employed to evaluate the neuron and axon damage.[29] In the control (SCI) group (**Figures 2f** and **S2**), the NF200 immunoreactivity near the injury site was lower, 32.3 ± 1.7% and 29.8 ± 16.2% decrease at day 1 and 28 post-injury, than that located distant from the traumatic lesion area (**Figure 2**j). Regarding the AcDX group, the NF200 intensity of peritraumatic area was 19.2 ± 1.9% lower than that located further from the traumatic lesion area at day 1 post-injury (**Figures 2g** and **2j**). When the time extended to 28 days post-injury, the NF200 intensity of peritraumatic area was only 3.9 ± 5.5% lower than that located further from the traumatic lesion area for the AcDX group (**Figures S4** and **2j**). In comparison with the SCI only group, a significant increase ($P < 0.05$ for both 1 and 28 days post-injury) in NF200 labeling adjacent to the injury site was observed for AcDX treated group, suggesting the continuous neuronal protection effect of AcDX microspheres.

Western blot analysis was used to further validate the immunofluorescence analysis (**Figure 2k**). A semi-quantitative comparison of Western blot images showed that the GFAP expression in the AcDX group was significantly ($P = 0.048$) reduced as compared to the SCI only group (**Figure 2l**). Besides GFAP, the AcDX treatment also significantly ($P = 0.014$) reduced the CD68 expression (activation of microglia) at day 1 post-injury. A comparison of the NF200 expression demonstrated that AcDX treatment significantly ($P = 0.019$) protected neurons at day 1 post-injury. The Western blot analysis

results is highly consistent with the immunohistochemical studies, suggesting that AcDX can inhibit the reactivity of injury-related proteins and protect the injured neurons.

These immunohistochemistry results collectively demonstrate that AcDX microspheres not only suppressed the astrogliosis and inflammation, but also protected neurons, making AcDX a promising biomaterial for SCI treatment. The neuroprotective effect in the spinal cord tissue contributed to the rapid recovery of walking motion as early as 1 week after administration. The histological data corroborated the functional recovery results, showing that AcDX microspheres can enhance the recovery of injured spinal cord. However, the mechanism of neuronal protection by AcDX microsphere is unclear. In the following content, we further studied the possible mechanism for the attractive neuroprotection effect offered by AcDX microspheres.

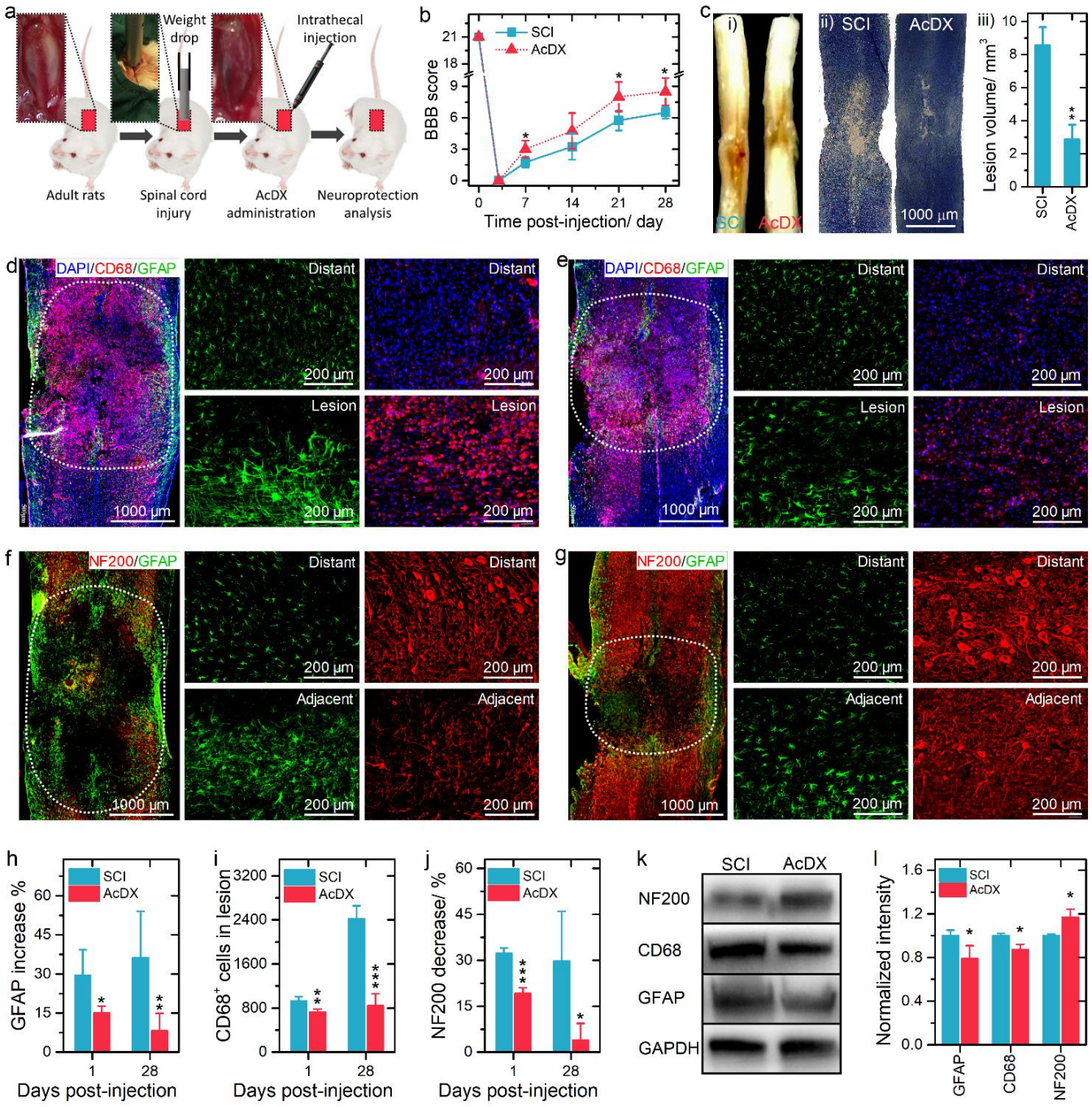

Figure 2. AcDX microspheres protect the traumatically injured spinal cord. (**a**) Schematic diagram of experimental design. AcDX microspheres were intrathecally injected within 5 min after weight drop at the T10 level. (**b**) The rats were functionally graded up to 28 days post-injury using the BBB grading scale (n = 5 animals per group). (**c**) Spinal cord at day 28 post-injury: (i) gross morphology, (ii) representative Nissl stained sagittal sections, and (iii) the lesion volumes (n = 3 animals per group). (**d** and **e**) Representative immunohistochemical staining images of GFAP (in green)

and CD68 (in red) in the spinal cord tissues of SCI (d) and AcDX (e) groups at day 1 post-injury. The boundary of cavity is indicated by the dashed lines. Right two columns are the enlarged images corresponding to the distant (> 10 mm) field to the lesion (upper row), and the lesion area (bottom row). The nuclei of all cells were stained with DAPI (in blue). (**f** and **g**) Representative immunohistochemical staining images of GFAP (in green) and NF200 (in red) in the injured spinal cord tissues of SCI (f) and AcDX (g) groups at day 1 post-injury. The dashed lines indicate the boundary of cavity. (**h-j**) Semi-quantification of GFAP intensity increase (h; $n \geq 5$ animals per group), the number of $CD68^+$ microglia in the traumatic lesion area (i; $n \geq 4$ animals per group), and NF200 intensity decrease (j; $n \geq 4$ animals per group). (**k**) Representative Western blots of NF200, CD68 and GFAP in lesion extracts at day 1 post-trauma. (**l**) Semi-quantification of relative expression level of NF200, CD68 and GFAP, normalized to GAPDH ($n = 3$ animals per group). Data present as mean ± s.d.; the levels of significance were set at probabilities of $^{*}P < 0.05$, $^{**}P < 0.01$, and $^{***}P < 0.001$.

Excitotoxicity is one of the most important pathological and neurochemical changes after SCI. Specifically, neurons are under the excessive stimulation by neurotransmitter GLU;[30] the high GLU concentration around the synaptic cleft induces the neuronal cell death. Neuron apoptosis contributes to the neuronal cell death and to the neurological dysfunction, induced by traumatic insults to the rat spinal cord.[31] We studied the neuronal apoptosis by propidium iodide (PI)/Hoechst 33342 (HC) staining (**Figure 3a**). The high intensity of PI indicates the cell death. HC staining was performed to visualize the nuclear morphology of neurons and to distinguish those apoptotic ones. The control neurons exhibited uniformly dispersed chromatin and intact cell membrane (PI-negative). The high magnification of neurons for each group is shown in **Figure S6**. After the administration of GLU, neurons exhibited typical characteristics of apoptosis, such as the condensation of chromatin, the shrinkage of nuclear, and the enhanced cell membrane permeability. We evaluated the neuroprotective

effect of AcDX microspheres on the GLU-induced excitotoxicity model. Three concentrations of AcDX microspheres, 0.25 mg/mL (AcDXL), 1.0 mg/mL (AcDXM) and 4.0 mg/mL (AcDXH), were selected for the following *in vitro* tests. Independent on the AcDX concentrations tested, the number of neurons with nuclear condensation and fragmentation decreased after AcDX microsphere treatment.

We further investigated the protection mode of AcDX microspheres by staining primary neurons with paired FITC-labelled annexin V (FAV; in green) and PI (in red), and then examined it by flow cytometry (**Figure 3b**). In terms of early apoptotic cells, there was a prolonged maintenance of membrane integrity and an externalization of phosphatidylserine to which the FAV could specifically bind. Live cells were negative for both stains, whereas early apoptotic cells were characterized by a high FAV signal in the absence of PI staining. The viability of neurons decreased to about 50% (**Figure 3c**) after GLU-induced excitotoxicity, about one third of neurons had lost membrane integrity (PI-positive; **Figure 3d**), and approximately 13% neurons were at the early apoptotic stage (FAV-positive and PI-negative; **Figure 3e**). Under the protection of AcDX microspheres, the viability of neurons was significantly improved ($P < 0.01$) for all three concentrations tested. As expected, the fraction of PI- and FAV-positive neurons significantly ($P < 0.01$) decreased when neurons were incubated with AcDX microspheres. The strongest protection effect was observed for the AcDXM group. The flow cytometry measurements were consistent with the fluorescence image analysis; both results indicated that AcDX microspheres can protect primary neurons from GLU-induced excitotoxicity.

Next, we analyzed the expression level of pro-apoptotic proteins (Calpain and Bax), anti-apoptotic protein (Bcl-2), and the apoptotic symbol caspases enzymes in primary neurons to preliminarily understand the mechanism of anti-apoptosis effect of AcDX microspheres (**Figure 3f**).[32] Among the caspases discovered, caspase-3 is an executioner of apoptosis, cleaving several essential downstream substrates.[33] Moreover, the activation of caspase-9, an important initiator of apoptosis, has been implicated in SCI.[34] The semi-quantitative analysis of Western blot images is presented in **Figure 3g**. Toward the GLU-induced excitotoxicity model, the significantly elevated expression level of Calpain

($P < 0.001$), Caspase-9 ($P = 0.011$) and Caspase-3 ($P = 0.003$), and Bax ($P = 0.004$) were observed in primary neurons, when compared to the PBS group. In contrast, the expression level of Bcl-2 notably decreased ($P < 0.001$) when GLU was added. After the administration of AcDX microspheres, the Western blot analyses revealed lower levels of Calpain and Caspase-9 and Caspase-3 than those of GLU group, whereas the expression of Bcl-2 improved. In terms of Bax, no significant difference was observed for the AcDXL and AcDXM groups when compared to the GLU group. The expression level of Bax for AcDXH was even significantly ($P = 0.002$) higher than that from the GLU group. The neuronal protection effect of AcDX microspheres can attributed to the attenuation of pro-apoptotic proteins (Calpain, Caspase-9 and Caspase-3) and the enhanced expression of anti-apoptotic protein (Bcl-2). Furthermore, the ratio of Bcl-2 to Bax is known as a key determinant of neuronal commitment to apoptosis.[35] Bcl-2/Bax increased for AcDX microspheres compared with GLU group, indicating that AcDX treatment inhibited the mitochondria-mediated cell death pathway.

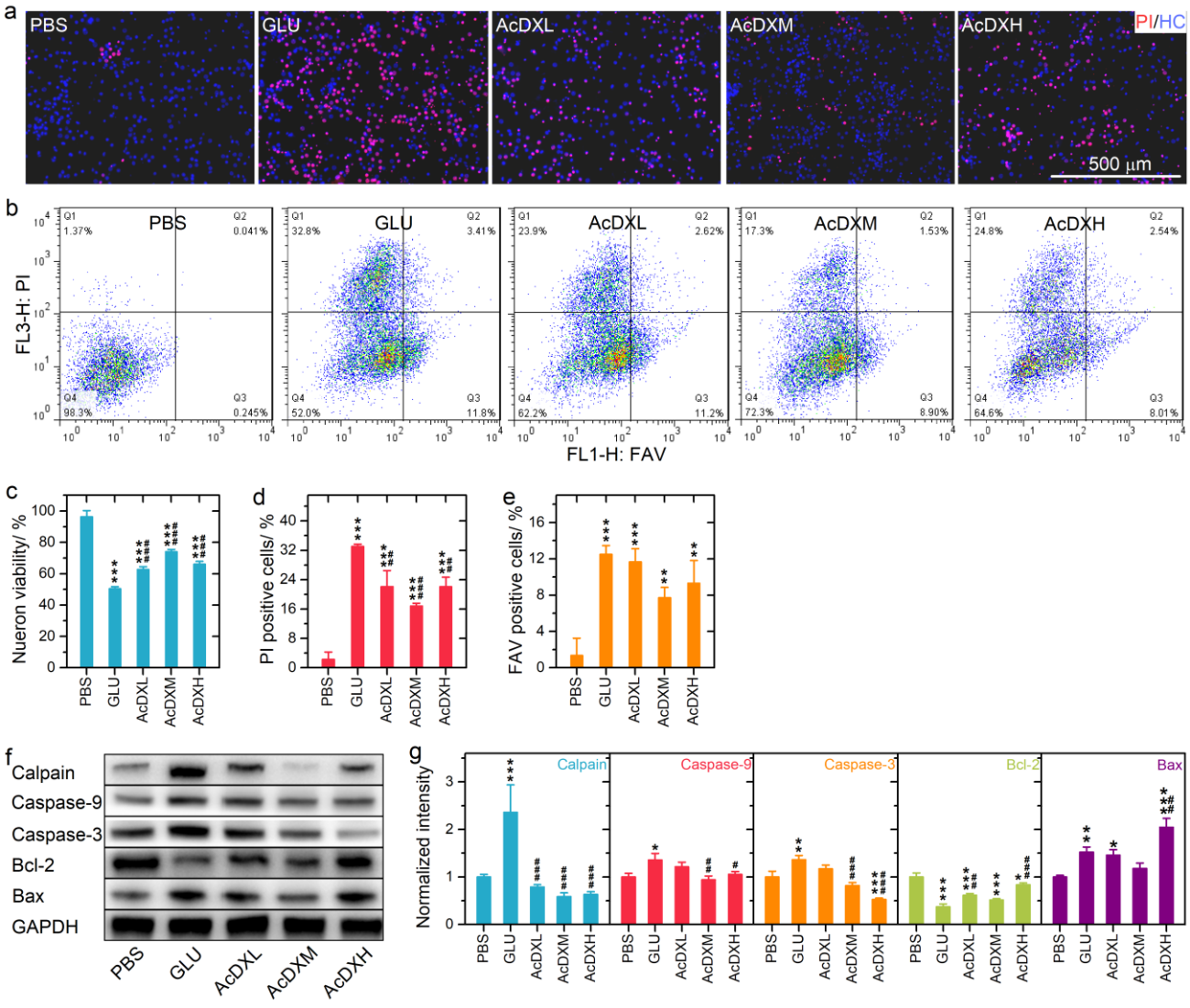

Figure 3. AcDX microspheres alleviate the GLU-induced neuronal apoptosis *in vitro*. For *in vitro* tests, the neurons were firstly incubated with microspheres for 15 min, followed by the administration of GLU (100 μM) for all the groups, except for the PBS one. (**a**) Representative fluorescence images of propidium iodide (PI, in red; marker of dead cells) and Hoechst 33342 (HC, in blue; nuclear marker for both survival and apoptotic cells) stained neurons incubated with AcDX microspheres after GLU-induced excitotoxicity. (**b**) Examples of scatter plots for neurons incubated with AcDX microspheres after GLU-induced excitotoxicity by PI/FAV double labeling. (**c**−**e**) Quantitative results of live (c), and PI- (d) and FAV-positive (e) neurons with and without the treatment by AcDX microspheres (n = 3). (**f**) Representative Western blot analysis of apoptosis indicated proteins in neurons incubated with AcDX microspheres after GLU-induced excitotoxicity. (**g**) Semi-quantification of relative expression

level of apoptosis indicated proteins in primary neurons, normalized to GAPDH (n = 3). The AcDX microspheres were compared with the groups of PBS (*) and GLU ($^{\#}$). Data present as mean ± s.d.; the levels of significance were set at probabilities of $^{*,\ \#}P < 0.05$, $^{**,\ \#\#}P < 0.01$, and $^{***,\ \#\#\#}P < 0.001$.

We assessed the extent of cell apoptosis in the peritraumatic zone of spinal cord by the terminal deoxynucleotidyl transferase-mediated dUTP nick end labeling (TUNEL) assay. The selected TUENL assay time point was 1 day post-injury, when a burst of neuronal and glial apoptosis in gray and white matter at the lesion site was observed.[31] The sagittal sections of the spinal cords treated with PBS and AcDX microspheres are presented in **Figure 4a**. High magnification of sagittal sections showed a clear cellular alteration of typical apoptosis, green colored and indicated by white arrows (**Figure S7**). On day 1 post-injury, the numbers of TUNEL-positive (apoptotic) cells for AcDX group was dramatically smaller (P = 0.006) than those treated with PBS (**Figure 4b**). The *in vivo* TUNEL assay confirmed that AcDX microspheres can effectively inhibit the cell apoptosis in the injured spinal cord, and these results are consistent with the *in vitro* tests.

The expression of apoptosis associated markers in the traumatic injured spinal cord was also evaluated by Western blot analysis (**Figure 4c**). The semi-quantitative comparison of Western blot images is shown in **Figure 4d**. The local delivery of AcDX microspheres prominently improved Bcl-2 (P = 0.022) expression and significantly reduced the expression level of Calpain (P < 0.001), Caspase-9 (P < 0.001), Caspase-3 (P = 0.012) and Bax (P = 0.002), as compared to the SCI only group. AcDX microspheres attenuated the pro-apoptotic proteins (Calpain, Caspase-9 and -3, and Bax) expression, and enhanced the expression of anti-apoptotic protein (Bcl-2), which corroborates the *in vitro* tests (**Figures 3f** and **3g**). In comparison to the SCI group, the higher Bcl-2/Bax ratio for the AcDX group indicates that the mitochondria-mediated cell death pathway in injured spinal cord can be blocked by AcDX spheres.

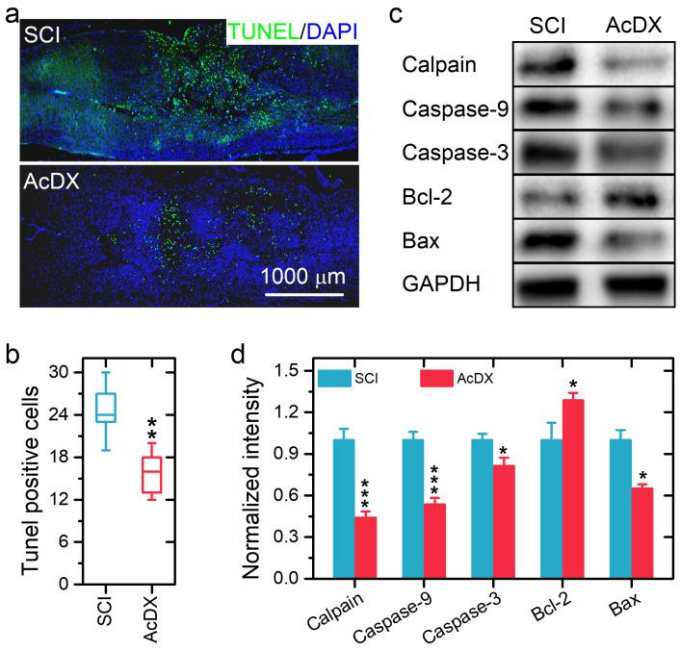

Figure 4. AcDX microspheres protect the injured neurons from apoptosis *in vivo*. (**a**) Representative images of TUNEL-positive apoptotic cells (in green) in sagittal spinal cord sections at day 1 post-trauma. The nuclei of all cells were stained with DAPI (in blue). (**b**) Comparison of the number of TUNEL-positive cells with and without AcDX microspheres treatment (n = 5 animals per group). (**c**) Representative Western blots of apoptosis indicated proteins in lesion extracts at day 1 post-trauma. (**d**) Semi-quantification of relative expression level of apoptosis indicated proteins, normalized to GAPDH. In terms of *in vivo* tests, the vehicle PBS served as the control (SCI group; n = 3 animals per group). Data present as mean ± s.d.; the levels of significance were set at probabilities of $^{*}P < 0.05$, $^{**}P < 0.01$, and $^{***}P < 0.01$.

In general, the pathologically high level of GLU can cause excitotoxicity by sustained calcium ion influx through GLU receptor channels, which is a common pathway of neuronal apoptosis.[36] We employed a calcium indicator, Fluo-4 AM ester, to monitor the intracellular calcium transients before and after the AcDX microsphere treatment.[37] Calcium influx by microscopy live imaging was determined over 5 min after establishing a baseline; F_0 is the baseline of Fluo-4 intensity and ΔF is the

change of Fluo-4 intensity in comparison to F_0. The time course of the Fluo-4 signals ($\Delta F/F_0$) as a function of time has been presented in **Figure 5a**. The GLU stimulation increased the peak intensity of Fluo-4 by approximately 5-fold, and peaked after approximately 2 min GLU stimulation. The incubation with ACDX microspheres before GLU stimulation effectively reduced the peak intensity of Fluo-4 for neurons. Specifically, the intracellular peak level of Fluo-4 reduced by approximately 30% (P = 0.041), 41% (P = 0.001) and 45% (P < 0.001) for AcDXL, AcDXM and AcDXH groups, respectively, in comparison with the GLU group (**Figure 5b**). After 5 min GLU stimulation, the Fluo-4 intensity difference was only observed between GLU and AcDXM (P = 0.019). **Figure 5c** shows the representative Fluo-4 fluorescence images of GLU-stimulated neurons incubated with different concentrations of AcDX microspheres. Overall, the neuronal protection effect of AcDX microspheres could be ascribed to the reduced calcium influx into neurons, which has also been observed for the poly(ethylene glycol)−poly(D,L-lactic acid) block copolymer.[7]

The high calcium ion loads increase the risk for mitochondrial damage, triggering the mitochondrial production of reactive oxygen species (ROS).[38] Hence, we monitored the intracellular ROS level to further corroborate the neuronal protection effect of AcDX microspheres.[39] The cell-permeant 2',7'-dichlorodihydrofluorescein diacetate (H_2DCFDA) was used as an indicator to detect the intracellular level of ROS in injured neurons. Oxidation of H_2DCFDA, forming highly fluorescent 2',7'-dichlorofluorescein (DCF), as determined using confocal microscopy was barely detectable in uninjured neurons (**Figure 5d**). The intensity of DCF fluorescence in GLU incubated neurons was markedly increased. Meanwhile, the administration of AcDX microspheres reduced the level of DCF fluorescence. The intensity changes of intracellular DCF fluorescence in different groups were confirmed by flow cytometry analysis (**Figures 5e** and **5f**). Based on the MFI values, only the intracellular ROS level for AcDXM group was notably (P < 0.05) lower than that of the GLU group.

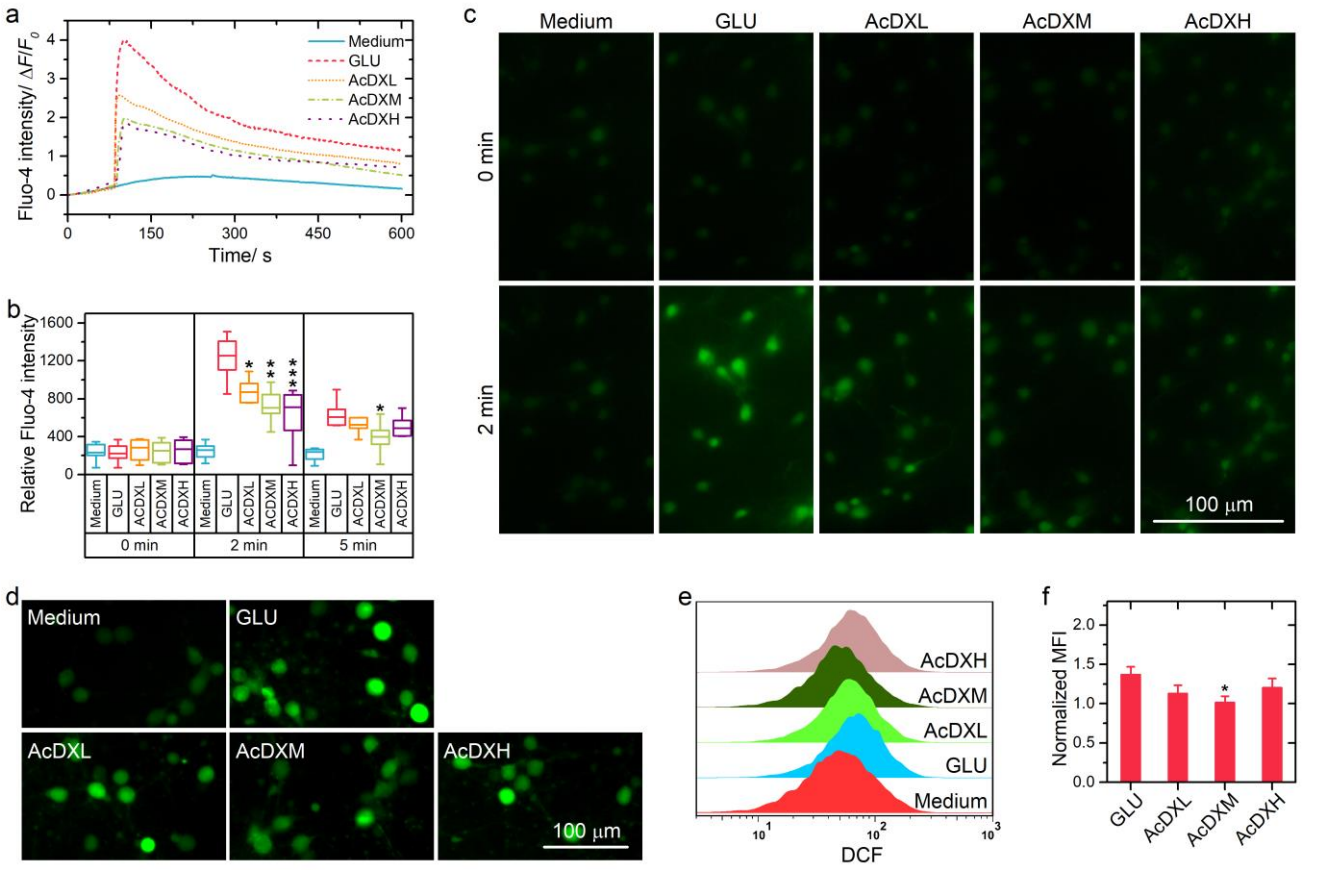

Figure 5. AcDX microspheres reduce the GLU-induced calcium ion influx and production of reactive oxygen species. (**a**) The time course of the Fluo-4 signals ($\Delta F/F_0$) as a function of time, with F_0 being the baseline Fluo-4 fluorescence and ΔF the change of Fluo-4 fluorescence in comparison to F_0. (**b**) Quantification of regions of interest demonstrating the effect of AcDX microspheres on reducing the fluorescence over time in response to GLU (n = 11). (**c**) Representative calcium images of neurons incubated with AcDX microspheres before (0 min) and after (2 min) GLU stimulation. (**d-f**) Representative ROS imaging (d), flow cytometry histograms (e), and the corresponding MFI (f; n = 3) of injured neurons incubated with AcDX microspheres. The MFI values were normalized to that of the PBS group. Data present as mean ± s.d.; the groups treated with AcDX microspheres were compared with the GLU group (*); the levels of significance were set at probabilities of $^{*}P < 0.05$, $^{**}P < 0.01$ and $^{***}P < 0.001$.

Lohmann *et al.*[40] synthesized glycosaminoglycan-based hydrogels, which can capture inflammatory chemokines to accelerate the wound healing. Inspiring by this inflammatory chemokine capture, we hypothesize that AcDX microspheres can alleviate the GLU-induced excitotoxicity through the physical adsorption of GLU. To verify this hypothesis, we evaluated the adsorption kinetics of GLU to AcDX microspheres, which was determined by incubation with 50 μM of GLU in artificial CSF (aCSF) As illustrated in **Figure 6a**, the more AcDX microsphere we added, the more GLU was adsorbed. For example, the adsorption of GLU up to about 6% was achieved, when the concentration of AcDX microspheres was 1 mg/mL. Moreover, the adsorption capacity of AcDXM and AcDXH for GLU was analyzed by incubating with a variety concentration of GLU in aCSF (25, 50 and 100 μM) for 30 min (**Figure 6b**). A linear correlation of the amounts of deployed and adsorbed GLU was found for both AcDXM and AcDXH. By increasing the GLU concentration from 25 to 100 μM, the percentage of GLU sequestered by AcDX microspheres decreased from 8% to 4% for AcDXM, and reduced from 22% to 10% for AcDXH.

We further verified the GLU capture capability of AcDX microspheres *in vivo* (**Figure 6c**). Detailed CSF sampling (100-150 μL) has been illustrated in **Video S1**. The GLU content in CSF was analyzed by an ultra-performance liquid chromatography and tandem mass spectrometry; a representative chromatogram of GLU in the CSF sample from the SCI only group at day 2 post-injury has been presented in **Figure S8**. Before injury, the GLU concentration in CSF is approximately 4 μM (t = day 0). For both SCI and AcDX groups, the GLU concentration in CSF continually increased until day 2 post-injury, and then decreased to a level (approximately 2 and 1 μM for SCI and AcDX, respectively) even lower than the normal GLU concentration (4 μM). Until day 4 post-injury, the GLU concentration for AcDX group was always significantly lower than that for the SCI only group. Specifically, after the administration of AcDX microspheres, the GLU concentration decreased from approximately 18 to 8 μM ($P < 0.05$) at 8 h post-injury, from approximately 77 to 58 μM ($P < 0.001$) at day 2 post-injury, and from approximately 64 to 53 μM ($P < 0.001$) at day 4 post-injury. We also calculated the area

under the curve (AUC) of GLU concentrations in CSF (**d**). The AUC of GLU for the group treated by AcDX microspheres was also significantly ($P < 0.01$) lower than that of the SCI only group. Based on both *in vitro* and *in vivo* GLU adsorption results, we can conclude that our AcDX microspheres can protect neurons from excitotoxicity by sequestering the GLU in CSF.

The overload of calcium ions is one of the most important features for the GLU-induced excitotoxicity, hence we also evaluated the adsorption capability of AcDX microspheres toward calcium ions. Surprisingly, the AcDX microspheres can also scavenge the calcium ions in aCSF (**Figure 6e**). This calcium ion scavenging capability of AcDXM and AcDXH was also confirmed by the relation between the deployed and adsorbed calcium ions (**Figure 6f**). Like the sequestering effect toward GLU in CSF, the administrated AcDX microspheres also reduced the intensity of the calcium ions in CSF (**Figure 6g**). In comparison to the SCI group, significantly lower calcium ion concentrations were observed at 8 h ($P < 0.05$), and day 1 ($P < 0.01$), 2 ($P < 0.001$) and 4 ($P < 0.001$) post-injury; the AUC of calcium ions for the group treated by AcDX microspheres was also significantly reduced ($P < 0.001$; **Figure 6h**). Therefore, the neuronal protection effect of AcDX microspheres can also be partially ascribed to their calcium ion scavenging feature.

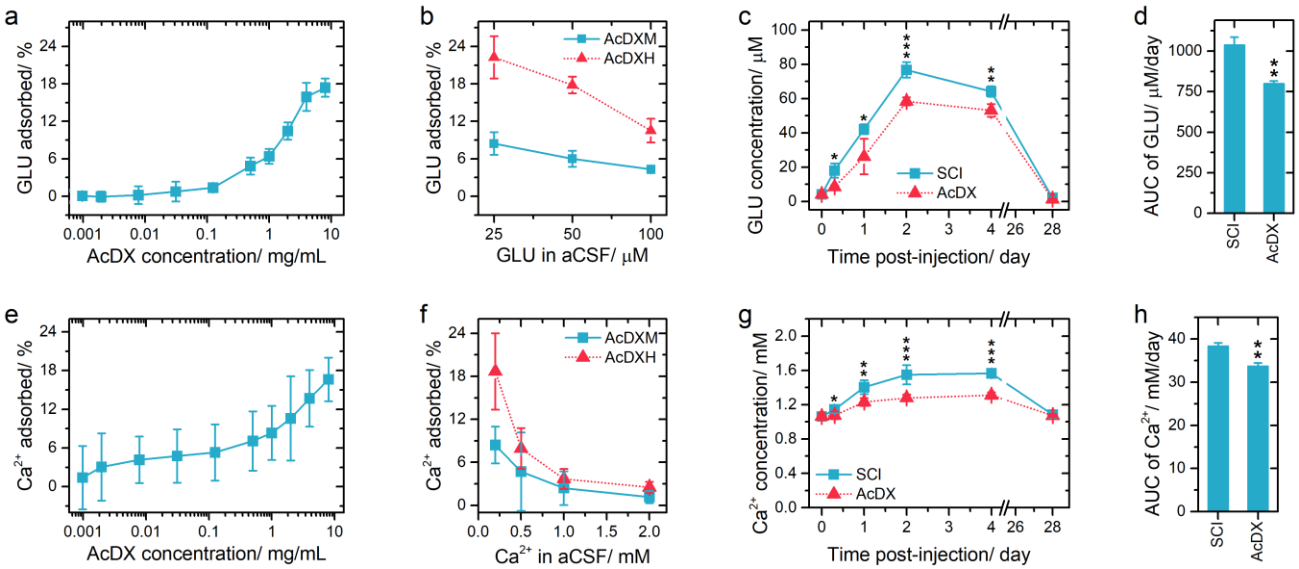

Figure 6. AcDX microspheres alleviate GLU-induced excitotoxicity by sequestering GLU and calcium ions. (**a**) The adsorption of GLU (50 μM) by AcDX microspheres in aCSF in terms of the microsphere concentrations (n = 6). (**b**) The impact of GLU concentrations on the adsorption of GLU by AcDX microspheres in aCSF (n = 6). (**c** and **d**) The effect of AcDX microspheres on the concentrations of GLU in the CSF as a function of time (c; $n \geq 3$ animals per time point) and the corresponding area under curve (d; n = 3). (**e**) The adsorption of calcium ions (0.5 mM) by AcDX microspheres in aCSF in terms of the microsphere concentrations (n = 6). (**f**) The impact of calcium ion concentrations on the adsorption of calcium ions by AcDX microspheres in aCSF (n = 6). (**g** and **h**) The effect of AcDX microspheres on the concentrations of calcium ions in the CSF as a function of time (g; $n \geq 3$ animals per time point) and the corresponding area under curve (h; n = 3). Data present as mean ± s.d.; the groups treated with AcDX microspheres were compared with the SCI only group (*); the levels of significance were set at probabilities of $^{*}P < 0.05$, $^{**}P < 0.01$ and $^{***}P < 0.001$.

GLU and calcium ions play a key role in excitotoxicity, which leads to neuronal cell apoptosis.[41] AcDX microspheres show the capability of buffering out excess GLU and calcium ions. Benefiting from the fast sequestering of GLU and calcium ions by AcDX microsphere, significantly lower level of GLU and calcium ions in CSF has been achieved at the first evaluation time point (8 h post-injury). By reducing the magnitude of the initial increase of extracellular GLU and calcium ions during the acute (2-48 h post-injury) and subacute (2-14 days post-injury) phases of SCI,[42] AcDX microspheres successfully attenuate the degree of excitotoxic secondary neuron damage. Like FITC-dextran and FITC (**Figure 1f**), the sequestered GLU and calcium ions will be released into CSF during the AcDX degradation process. Based on the degradation rate of AcDX microspheres, GLU and calcium ions being released from microspheres is unlikely to be cytotoxic, especially at the acute and subacute phases of SCI. During the chronic phase of SCI, the cellular mitochondrial storage, and astrocytic

connections to the vascular system through the blood brain barrier would work to prevent the reestablishment of cytotoxic level of GLU and calcium ions.[43] Our finding implies that AcDX microspheres should be administrated as soon as possible following the initial injury to maximize their therapeutic efficacy. These results provide an interesting potential drug delivery application for our microspheres during the acute/subacute phase of SCI.

This study demonstrates that the intrathecal administration of bare AcDX microspheres can protect neurons from GLU-induced excitotoxicity, and therefore, repair the injured spinal cord. The neuroprotective feature of AcDX microspheres is achieved by sequestering GLU and calcium ions in CSF, reducing the calcium ions influx into neurons and inhibiting the formation of ROS. Consequently, AcDX microspheres attenuate the expression of pro-apoptotic proteins (Calpain and Bax) and enhance the expression of anti-apoptotic protein (Bcl-2) both *in vitro* and *in vivo*. The intrathecal administration of AcDX microspheres immediately after traumatic injury leads to histological protection in spinal tissue and functional recovery in live animals. The administration of such microspheres or scaffolds may play an important role in the design of future strategies for the treatment of traumatic central nervous system injury, not limited to SCI. For example, benefiting from the protection effect of AcDX, the incorporation of therapeutic compounds into the AcDX-based drug delivery systems and scaffolds may bring synergistic outcome toward the SCI therapy and the treatment of other traumatic central nervous system injury. Follow-up studies will aim to load therapeutics into the AcDX microspheres to further improve the recovery of the injured spinal cord. In summary, our work opens an exciting perspective toward the application of neuroprotective AcDX for the treatment of severe neurological diseases.

Supporting Information

Experimental section and supporting figures are enclosed in Supporting Information, which is available from the Wiley Online Library or from the authors.

Acknowledgements

D. Liu, J. Chen and T. Jiang contributed equally to this work. We acknowledge financial support from the Academy of Finland (Grant Nos. 308742, 252215 and 281300), Jane and Aatos Erkko Foundation (No. 4704010), Research Funds of the University of Helsinki, the European Research Council under the European Union's Seventh Framework Programme (FP/2007-2013, No. 310892), the National Natural Science Foundation of China (Grant Nos. 81772352, 81401807, 81772351 and 81271988), and Natural Science Foundation of Jiangsu Province (Grant No. BK2012876).

Received: ((will be filled in by the editorial staff))

Revised: ((will be filled in by the editorial staff))

Published online: ((will be filled in by the editorial staff))

Table of Contents

Intrathecally administrated acetalated dextran microspheres scavenge the glutamate and calcium ions in cerebrospinal fluid, attenuate the glutamate-induced excitotoxicity, and ultimately protect the injured spinal cord neurons in rats.

Keyword: spinal cord injury, acetalated dextran, neuroprotection, functional recovery, anti-apoptosis

Dongfei Liu, Jian Chen, Tao Jiang, Wei Li, Yao Huang, Xiyi Lu, Zehua Liu, Weixia Zhang, Zheng Zhou, Qirui Ding, Hélder A. Santos*, Guoyong Yin*, Jin Fan*

Biodegradable Spheres Protect Traumatically Injured Spinal Cord by Alleviating the Glutamate-Induced Excitotoxicity

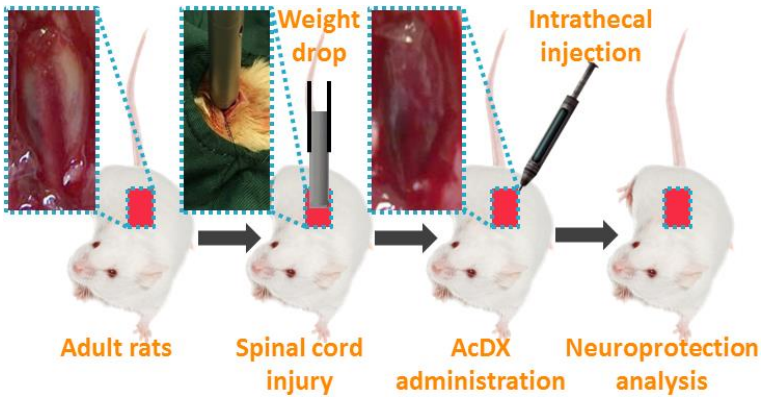

References:

[1] A. E. M. Mautes, M. R. Weinzierl, F. Donovan, L. J. Noble, Phys. Ther. 2000, 80, 673.

[2] a) S. B. Jazayeri, S. Beygi, F. Shokraneh, E. M. Hagen, V. Rahimi-Movaghar, Eur. Spine J. 2015, 24, 905; b) S. Thuret, L. D. Moon, F. H. Gage, Nat. Rev. Neurosci. 2006, 7, 628.

[3] D. D. French, R. R. Campbell, S. Sabharwal, A. L. Nelson, P. A. Palacios, D. Gavin-Dreschnack, J. Spinal Cord Med. 2007, 30, 477.

[4] A. K. Varma, A. Das, G. Wallace, J. Barry, A. A. Vertegel, S. K. Ray, N. L. Banik, Neurochem. Res. 2013, 38, 895.

[5] S. Kabu, Y. Gao, B. K. Kwon, V. Labhasetwar, J. Control. Release 2015, 219, 141.

[6] a) H. F. Wu, J. S. Cen, Q. Zhong, L. M. Chen, J. Wang, D. Y. B. Deng, Y. Wan, Biomaterials 2013, 34, 1686; b) D. Liu, T. Jiang, W. Cai, J. Chen, H. Zhang, S. Hietala, H. l. A. Santos, G. Yin, J. Fan, Adv. Healthc. Mater. 2016, 5, 1513.

[7] Y. Z. Shi, S. Kim, T. B. Huff, R. B. Borgens, K. Park, R. Y. Shi, J. X. Cheng, Nat. Nanotechnol. 2010, 5, 80.

[8] W. Wu, S. Y. Lee, X. Wu, J. Y. Tyler, H. Wang, Z. Ouyang, K. Park, X. M. Xu, J. X. Cheng, Biomaterials 2014, 35, 2355.

[9] a) G. C. de Ruiter, R. J. Spinner, M. J. A. Malessy, M. J. Moore, E. J. Sorenson, B. L. Currier, M. J. Yaszemski, A. J. Windebank, Neurosurgery 2008, 63, 144; b) J. R. Slotkin, C. D. Pritchard, B. Luque, J. Ye, R. T. Layer, M. S. Lawrence, T. M. O'Shea, R. R. Roy, H. Zhong, I. Vollenweider, V. R. Edgerton, G. Courtine, E. J. Woodard, R. Langer, Biomaterials 2017, 123, 63.

[10] S. F. Wang, D. H. Kempen, N. X. Simha, J. L. Lewis, A. J. Windebank, M. J. Yaszemski, L. C. Lu, Biomacromolecules 2008, 9, 1229.

[11] B. K. K. Chen, A. M. Knight, N. N. Madigan, L. Gross, M. Dadsetan, J. J. Nesbitt, G. E. Rooney, B. L. Currier, M. J. Yaszemski, R. J. Spinner, A. J. Windebank, Biomaterials 2011, 32, 8077.

[12] W. T. Daly, A. M. Knight, H. Wang, R. de Boer, G. Giusti, M. Dadsetan, R. J. Spinner, M. J. Yaszemski, A. J. Windebank, Biomaterials 2013, 34, 8630.

[13] E. M. Bachelder, T. T. Beaudette, K. E. Broaders, J. Dashe, J. M. Frechet, J. Am. Chem. Soc. 2008, 130, 10494.

[14] K. E. Broaders, J. A. Cohen, T. T. Beaudette, E. M. Bachelder, J. M. Frechet, Proc. Natl. Acad. Sci. USA 2009, 106, 5497.

[15] a) S. L. Suarez, A. Munoz, A. C. Mitchell, R. L. Braden, C. L. Luo, J. R. Cochran, A. Almutairi, K. L. Christman, ACS Biomater. Sci. Eng. 2016, 2, 197; b) S. Suarez, G. N. Grover, R. L. Braden, K. L. Christman, A. Amutairi, Biomacromolecules 2013, 14, 3927.

[16] J. W. McDonald, C. Sadowsky, Lancet 2002, 359, 417.

[17] S. Y. Teh, R. Lin, L. H. Hung, A. P. Lee, Lab Chip 2008, 8, 198.

[18] a) W. Li, D. Liu, H. Zhang, A. Correia, E. M. Mäkilä, J. Salonen, J. T. Hirvonen, H. A. Santos, Acta Biomater. 2017, 48, 238; b) D. Liu, H. Zhang, B. r. Herranz-Blanco, E. M. Mäkilä, V.-P. Lehto, J. Salonen, J. T. Hirvonen, H. l. A. Santos, Small 2014, 10, 2029; c) D. Liu, B. Herranz-Blanco, E. M. Mäkilä, L. R. Arriaga, S. Mirza, D. A. Weitz, N. Sandler, J. Salonen, J. T. Hirvonen, H. A. Santos, ACS Appl. Mater. Inter. 2013, 5, 12127.

[19] R. Vasiliauskas, D. Liu, S. Cito, H. Zhang, M. A. Shahbazi, T. Sikanen, L. Mazutis, H. A. Santos, ACS Appl. Mater. Inter. 2015, 7, 14822.

[20] Y. L. Lai, P. M. Smith, W. J. Lamm, J. Hildebrandt, J. Appl. Physiol. Respir. Environ. Exerc. Physiol. 1983, 54, 1754.

[21] P. R. Wich, J. M. J. Frechet, Aust. J. Chem. 2012, 65, 15.

[22] R. Di Terlizzi, S. Platt, Vet. J. 2006, 172, 422.

[23] J. C. Bresnahan, M. S. Beattie, F. D. Todd, D. H. Noyes, Exp. Neurol. 1987, 95, 548.

[24] M. T. Fitch, J. Silver, Exp. Neurol. 2008, 209, 294.

[25] J. C. Fleming, M. D. Norenberg, D. A. Ramsay, G. A. Dekaban, A. E. Marcillo, A. D. Saenz, M. Pasquale-Styles, W. D. Dietrich, L. C. Weaver, Brain 2006, 129, 3249.

[26] M. E. Schwab, Science 2002, 295, 1029.

[27] S. Papa, I. Caron, E. Erba, N. Panini, M. De Paola, A. Mariani, C. Colombo, R. Ferrari, D. Pozzer, E. R. Zanier, F. Pischiutta, J. Lucchetti, A. Bassi, G. Valentini, G. Simonutti, F. Rossi, D. Moscatelli, G. Forloni, P. Veglianese, Biomaterials 2016, 75, 13.

[28] A. Petzold, J. Neurol. Sci. 2005, 233, 183.

[29] R. Posmantur, R. L. Hayes, C. E. Dixon, W. C. Taft, J. Neurotrauma 1994, 11, 533.

[30] O. N. Hausmann, Spinal Cord 2003, 41, 369.

[31] X. Z. Liu, X. M. Xu, R. Hu, C. Du, S. X. Zhang, J. W. McDonald, H. X. Dong, Y. J. Wu, G. S. Fan, M. F. Jacquin, C. Y. Hsu, D. W. Choi, J. Neurosci. 1997, 17, 5395.

[32] D. W. Nicholson, N. A. Thornberry, Trends Biochem. Sci. 1997, 22, 299.

[33] J. E. Springer, R. D. Azbill, P. E. Knapp, Nat. Med. 1999, 5, 943.

[34] S. Krajewski, M. Krajewska, L. M. Ellerby, K. Welsh, Z. Xie, Q. L. Deveraux, G. S. Salvesen, D. E. Bredesen, R. E. Rosenthal, G. Fiskum, J. C. Reed, Proc. Natl. Acad. Sci. USA 1999, 96, 5752.

[35] J. Qiu, O. Nesic, Z. Ye, H. Rea, K. N. Westlund, G. Y. Xu, D. McAdoo, C. E. Hulsebosch, J. R. Perez-Polo, J. Neurotrauma 2001, 18, 1267.

[36] a) X. X. Dong, Y. Wang, Z. H. Qin, Acta Pharmacol. Sin. 2009, 30, 379; b) M. Ankarcrona, J. M. Dypbukt, E. Bonfoco, B. Zhivotovsky, S. Orrenius, S. A. Lipton, P. Nicotera, Neuron 1995, 15, 961; c) J. F. Stover, A. W. Unterberg, Brain Res. 2000, 875, 51.

[37] a) C. Grienberger, A. Konnerth, Neuron 2012, 73, 862; b) M. M. Harraz, S. M. Eacker, X. Q. Wang, T. M. Dawson, V. L. Dawson, Proc. Natl. Acad. Sci. USA 2012, 109, 18962.

[38] A. Atlante, P. Calissano, A. Bobba, S. Giannattasio, E. Marra, S. Passarella, FEBS Lett. 2001, 497, 1.

[39] A. C. Rego, C. R. Oliveira, Neurochem. Res. 2003, 28, 1563.

[40] N. Lohmann, L. Schirmer, P. Atallah, E. Wandel, R. A. Ferrer, C. Werner, J. C. Simon, S. Franz, U. Freudenberg, Sci. Transl. Med. 2017, 9.

[41] C. A. Oyinbo, Acta Neurobiol. Exp. 2011, 71, 281.

[42] R. G. Grossman, R. F. Frankowski, K. D. Burau, E. G. Toups, J. W. Crommett, M. M. Johnson, M. G. Fehlings, C. H. Tator, C. I. Shaffrey, S. J. Harkema, J. E. Hodes, B. Aarabi, M. K. Rosner, J. D. Guest, J. S. Harrop, J. Neurosurg. Spine 2012, 17, 119.

[43] a) D. K. Anderson, L. D. Prockop, E. D. Means, L. E. Hartley, J. Neurosurg. 1976, 44, 715; b) N. J. Olby, N. J. H. Sharp, K. R. Munana, M. G. Papich, J. Neurotrauma 1999, 16, 1215.

Submitted to ADVANCED MATERIALS

DOI: 10.1002/adma.(please add manuscript number)

Biodegradable Spheres Protect Traumatically Injured Spinal Cord by Alleviating the Glutamate-Induced Excitotoxicity

By Dongfei Liu, Jian Chen, Tao Jiang, Wei Li, Yao Huang, Xiyi Lu, Zehua Liu, Weixia Zhang, Zheng Zhou, Qirui Ding, Hélder A. Santos*, Guoyong Yin*, Jin Fan*

Dr. D. Liu, Dr. W. Li, Z. Liu and Prof. H. A. Santos
Division of Pharmaceutical Chemistry and Technology
Faculty of Pharmacy, University of Helsinki
FI-00014, Helsinki, Finland.
Email: helder.santos@helsinki.fi (H. A. Santos)

Dr. D. Liu and Prof. H. A. Santos
Helsinki Institute of Life Science
HiLIFE, University of Helsinki
FI-0014 Helsinki, Finland

Dr. D. Liu and Dr. W. Zhang
John A. Paulson School of Applied Science and Engineering
Harvard University
MA 02138, Cambridge, USA.

J. Chen, T. Jiang, Y. Huang, Z. Zhou, Q. Ding, Prof. G. Yin and Prof. J. Fan
Department of Orthopaedics
The First Affiliated Hospital of Nanjing Medical University
Nanjing 210029, China
Email: guoyong_yin@sina.com (G. Yin) and fanjin@njmu.edu.cn (J. Fan)

T. Jiang
Department of Orthopaedics

Wuxi People's Hospital Affiliated to Nanjing Medical University
Wuxi 214023, China

X. Lu
Department of Oncology
The First Affiliated Hospital of Nanjing Medical University
Nanjing 210029, China.

Keywords: acetalated dextran; spinal cord injury; alleviated excitotoxicity; glutamate adsorption; calcium ion scavenging

Spinal cord injury (SCI) is the result of an initial mechanical disruption in the spinal cord structures (primary insult), followed by a secondary event that collectively injures the intact neighboring tissue.[1] Worldwide, an estimated 2.5 million people are living with SCI, with more than 130 thousand new injuries reported annually.[2] Traumatic SCI is a debilitating injury that have a life-long impact on the injured person. The economic cost of SCI is estimated to be approximately 9.7 billion dollars annually in the United States.[3] Despite its significant societal and economic impacts, few clinical treatments exist for traumatic SCI, and they only have limited therapeutic efficacy.[4] Therefore, new therapeutic strategies with improved therapeutic efficacy have been actively pursued.[5]

One of the promising approaches to treat traumatic SCI is using biomaterials. Several biodegradable polymers have been illustrated to support or promote axon regeneration in central nervous system. For example, the local administration of hydrogel composing of poloxamers (nonionic amphiphilic triblock copolymers) has been shown to slightly improve the functional motor recovery of injured spinal cord.[6] The self-assembled poly(ethylene glycol)−poly(D,L-lactic acid) block copolymer micelles repair the injured axonal membranes and reduce the calcium influx into axons, resulting in an improvement of locomotor function after traumatic SCI in adult rats.[7] Functional restoration of injured spinal cord has also been observed through the intravenously administration of ferulic acid modified glycol chitosan nanoparticles at 2 h post-injury.[8] Moreover, poly(lactic-co-glycolic acid),[9] poly(caprolactone fumarate)[10] and oligo[(polyethylene glycol) fumarate][11] have previously been shown to benefit the neuron repair.[12]

Recently, a biodegradable water-insoluble polymer ‘acetalated-dextran’ (AcDX) was synthesized by modifying hydroxyl groups of water-soluble dextran with 2-methoxypropene.[13] Because of its high solubility in organic solvents, AcDX and its derivatives have been formulated into micro- and nano-particles for biomedical applications, such as immunotherapy[14] and myocardial infarction treatment.[15] The immunogenicity of subunit vaccines could be enhanced by encapsulating a protein antigen and/or adjuvant within AcDX microspheres.[14] AcDX microspheres loaded with an engineered

hepatocyte growth factor fragment were employed for the treatment of myocardial infarction.[15] The cardioprotective efficacy of payload was optimal when delivered over 3 days post-intramyocardial injection, yielding the largest arterioles and the fewest apoptotic cardiomyocytes bordering the infarct.[15a]

After SCI, glutamate (GLU) floods out of injured spinal neurons, axons, and astrocytes, overexciting neighboring neurons.[16] The overexcited cells let in waves of calcium ions, which can trigger a series of destructive events, including production of highly reactive free radicals. These radicals can attack membranes and other cell organelles, and result in the neuronal death. These processes inevitably aggravate the injury of spinal cord. Hence, capturing GLU at the acute phase of injury may offer new treatment modalities for SCI therapy. In this study, we found out that the polymer AcDX itself can protect the injured spinal cord by reducing the level of GLU in cerebrospinal fluid (CSF) within hours after injection, and therefore, inhibit the GLU-induced excitotoxicity. Specifically, the intrathecally injected AcDX microspheres reduced the traumatic lesion volume, inhibited inflammatory response, protected the spinal cord neurons, and ultimately showed the improved locomotor function following traumatic SCI.

The synthesis approach of AcDX is shown in **Figure 1a**.[13] In the presence of an acid catalyst (*p*-toluenesulfonate), the modification of vicinal diols with 2-methoxypropene efficiently transformed the water soluble dextran into water insoluble AcDX.[14] Based on the ^{1}H nuclear magnetic resonance (NMR; **Figure 1b**) spectrum of AcDX, the calculated conjugation ratio was approximately 80.4%, corresponding to 48 out of 60 glucose units in a dextran (MW 10,000 g/mol) modified by 2-methoxypropene. Fourier transform infrared (FTIR; **Figure 1c**) spectra showed a clear intensity decrease of the O-H stretch at 3325 cm^{-1}, which can be ascribed to the reaction of vicinal diols with 2-methoxypropene.

Microfluidic technology provides an easy-to-use approach for the preparation of monodisperse droplets.[17] The obtained AcDX were formulated into microspheres using a microfluidic flow-

focusing device (**Figure 1d**).[18] The device was composed of two types of capillaries for which the outer diameter (about 1.0 mm) of the cylindrical tapered capillary fitted the inner dimension (about 1.1 mm) of the outer capillary. The inner oil fluid was an AcDX ethyl acetate solution (20 mg/mL) and the outer aqueous fluid contained amphiphilic Poloxamer 407 (10 mg/mL). The oil and aqueous fluids were simultaneously pumped into the microfluidic device in the opposite directions. This flow-focusing geometry forced the inner oil fluid to breakdown, forming single O/W emulsion drops at the orifice of the inner capillary. All the collected droplets were solidified through the diffusion of ethyl acetate to the external aqueous phase. As shown in the scanning electron microscope (SEM) image (**Figure 1e-i**), the obtained AcDX microspheres are all spherical. Toward the fluorescein isothiocyanate (FITC)-loaded AcDX microspheres, the fluorescence intensity distribution within microspheres was uniform (**Figure 1e-ii**), indicating a solid structure of the obtained microspheres.[19] We can see from **Figure 1e-iii**, the average particle size of AcDX microspheres was approximately 7.2 μm with a narrow size distribution (polydispersity index = 11.1%, defined as the ratio between the standard deviation and the mean diameter of particles multiplied by 100%).

To monitor the degradation behavior of AcDX microspheres, the FITC-labelled AcDX was synthesized by modifying the vicinal diols of FITC-labelled dextran with 2-methoxypropene. At pH 7.4, AcDX decomposed slowly through hydrolyzation of the acetals, regenerating the water-soluble FITC-dextran over a period of 50 days (**Figure 1f**).[15b] This degradation of AcDX microspheres is further reflected in the release profile of a model payload, FITC (**Figure 1f**). The release of FITC from AcDX microspheres was faster than that of FITC-dextran, which was only observed after 8 days of incubation. These two release profiles suggest that the payload only diffused out when the microspheres degraded, as opposed to passive diffusion through the intact microspheres. To corroborate these results, the degradation of AcDX microspheres was visualized using SEM. The morphology of the AcDX microspheres at day 1, 7, and 28 is shown in **Figure 1g**. The increased surface roughness is clearly visible for AcDX microspheres at day 1 and 7. After 1 month of incubation

at pH 7.4, most of the polymer matrix for AcDX microspheres was degraded. These SEM images correlate well with the observed FITC and FITC-dextran release profiles.

We evaluated the cytocompatibility (activity of dehydrogenases) of AcDX microspheres with primary neurons (**Figure 1h**). No obvious cytotoxicity was observed for AcDX microspheres within the tested concentration range (0.1−4.0 mg/mL) and the selected incubation time (6−96 h). Interestingly, enhanced neuron activity was observed after incubating with AcDX microspheres for 24, 48 and 72 h. After 24 h incubation, notable neuron viability enhancement was only observed for the highest concentration of AcDX microspheres (4.0 mg/mL). When the incubation time was extended to 48 h, remarkable cell viability increase was observed for AcDX microspheres with a concentration as low as 0.2 mg/mL. The cell viability enhancement effect for AcDX microspheres disappeared after increasing the incubation time to 96 h, which could be ascribed to the accumulation of by-products of cellular metabolism inside the medium. The cytocompatibility test suggests the neuroprotective effect of AcDX microspheres, especially within the concentration range of 0.2−4.0 mg/mL.

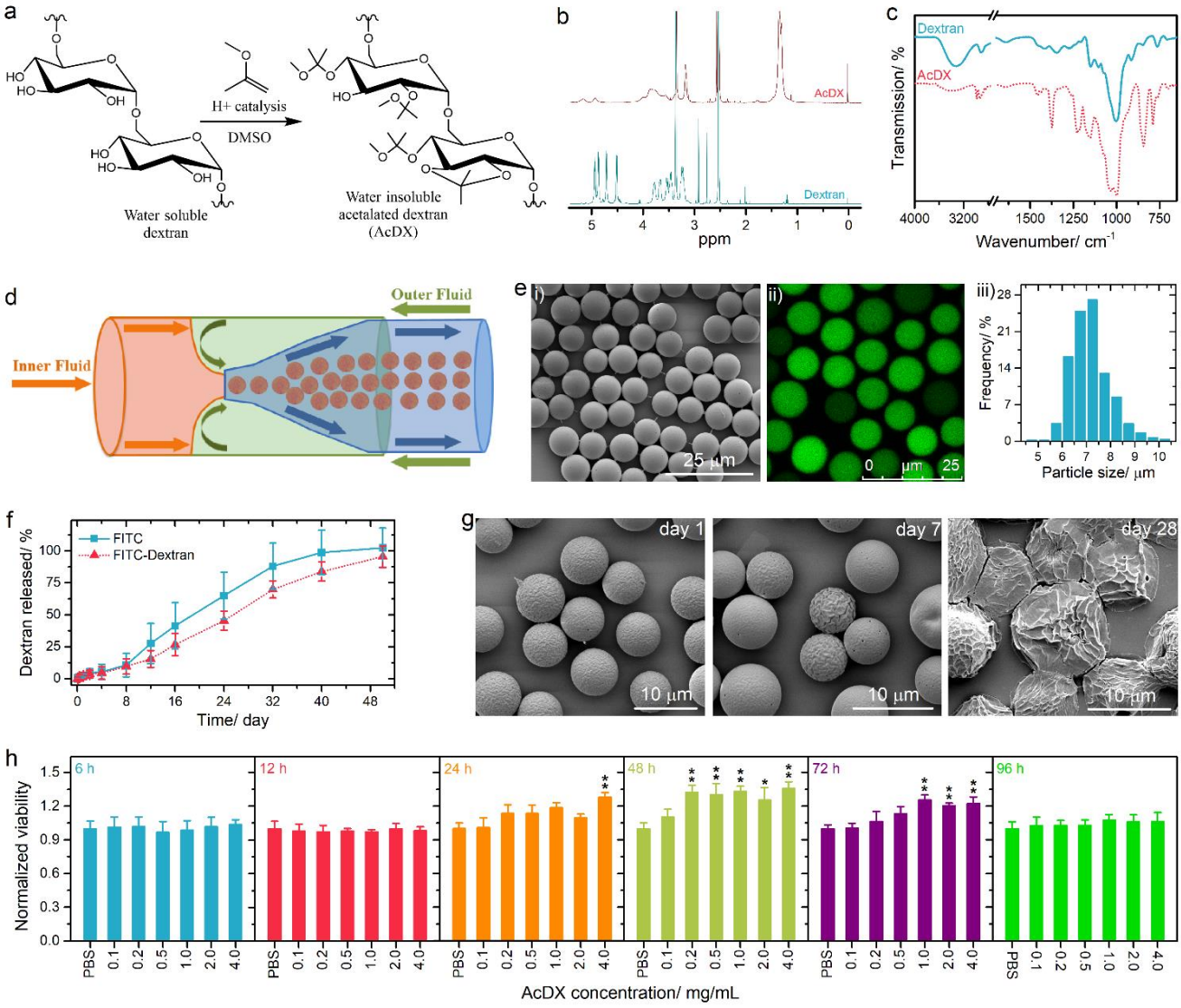

Figure 1. Preparation and characterization of AcDX microspheres and their neuronal compatibility. (**a-c**) Single-step synthesis of AcDX (a), and its NMR (b) and FTIR (c) spectra. (**d**) A schematic diagram of AcDX microspheres prepared by droplet microfluidics. (**e**) SEM (i) and confocal fluorescence microscopy (ii) images of the obtained AcDX microspheres, and their size distribution (iii). (**f**) Dissolution of FITC-dextran and FITC from AcDX microspheres in 1 × phosphate-buffered saline (1 × PBS, pH 7.4) at 37 °C (n = 3). (**g**) SEM images of AcDX microspheres after 1, 7 and 28 days of incubation in PBS (pH 7.4) at 37 °C. (**h**) The effect of AcDX microspheres (0.1-4.0 mg/mL) on the viability of primary neurons (n = 5). The neuronal viabilities incubated with AcDX

microspheres were compared with that of the PBS group. Data present as mean ± s.d.; the levels of significance were set at probabilities of $^{*}P < 0.05$ and $^{**}P < 0.01$.

To verify the neuroprotective effect of AcDX microspheres, we performed a functional motor assessment and histological injury study in Sprague-Dawley rats undergoing a weight-drop injury of the thoracic spinal cord (T10; **Figure 2**a). Regarding all the *in vivo* test, AcDX microspheres (60 μg/μL, 10 μL in total) were intrathecally administrated within 5 min post-injury. Because the cerebrospinal fluid volume in rat brain is approximately 580 μL,[20] the theoretical total volume would be approximately 590 μL after the administration of AcDX microspheres. Therefore, the final AcDX concentration (600 μg in 590 μL) achieved about 1 mg/mL, which was proved to be effective in neuron viability enhancement (**Figure 1h**). The vehicle PBS served as the control (SCI group). The degradation rate of AcDX is primarily controlled by the pH value of the incubation medium.[21] After intrathecally administration, the AcDX microspheres were dispersed in CSF. In general, CSF is clear, colorless, nearly acellular, and has a low protein concentration.[22] Since the component, especially the pH value, of CSF is similar to the *in vitro* incubation medium, the *in vivo* degradation rate of AcDX is also expected to be close to that observed *in vitro*. Instead of breaking into smaller pieces, AcDX microspheres presented an "outside-in" pattern of degradation (**Figure 1**g). Their degradation pattern indicates that AcDX microspheres would remain inside the CSF before complete degradation.

After traumatic SCI, the motor behavior was assessed by the 21-point Basso, Beattie, and Bresnahan (BBB) locomotor rating scale in open-field (**Figure 2b**). The complete hindlimb paralysis (BBB score = 0) was observed for both SCI and AcDX groups at day 1 post-injury. At day 7 post-injury, the AcDX group showed extensive movement of two joints (BBB score = 3.0 ± 0.8), which is significantly (P = 0.040) higher than the locomotor performance of SCI group (BBB score = 1.8 ± 0.5) with the extensive movement of only one joint. This superiority on the locomotor function for the AcDX group

maintained over the remainder of the motor assessment study. At day 28 post-injury, the plantar support of the paw with weight bearing only in the support stage was observed for the AcDX group with a score of 8.5 ± 1.3 on the BBB scale, whereas non-treated rats were approximately 2 points lower ($P < 0.05$). Overall, AcDX significantly improved the recovery of hindlimb motor function. In terms of the BBB score for the SCI group, it increased from 0 at day 1 post-injury to 6.5 ± 0.6 at day 28 after SCI, indicating a certain degree of spontaneous motor function recovery. This spontaneous locomotor function recovery was also included in the result of the AcDX group.

As shown by the gross morphology of the injured spinal cords, the traumatic lesion area (brown colored region) on the spinal cord was visible (**Figure 2c**). After treatment with AcDX microspheres, the lesion area was notably smaller than that of the SCI only group. A prominent pathological feature of SCI is the development of a fluid-filled cystic cavity that is bordered by reactive astrocytes.[23] The traumatic lesion cavity was identified by loss of cells using Nissl staining to study whether AcDX microspheres could reduce the lesion volume. Four weeks after injury, dramatic tissue loss on the injured spinal cord was observed (**Figure 2c**). The administration of AcDX microspheres caused a reduction in post-traumatic spinal cord tissue loss. Lesion volume was assessed by the Nissl-stained spinal cord sections, which sampled serially in the longitudinal plane with an interval of about 200 μm for each layer. As demonstrated in **Figure 2**c, the administration of AcDX microspheres significantly decreased ($P = 0.002$) the lesion volume (2.9 ± 0.9 mm^3) compared to the SCI control group (8.6 ± 1.1 mm^3).

To further understand the anatomical basis of the observed locomotor recovery, we examined the density or status of astrocytes, microglia, neurons, and axons. These cells play crucial roles in the spinal cord damage and repair. The cellular hypertrophy and increases in glial fibrillary acidic protein (GFAP) are hallmarks of astrocyte reactivity after SCI.[24] The injured spinal cord is also featured with enhanced numbers of activated Cluster of Differentiation 68 (CD68)-immunoreactive microglia.[25]

The reactive astrocytes and microglia were visualized using GFAP and CD68 immunofluorescence antibodies, respectively.

Regarding the non-treatment (SCI) group, the region in proximity to the lesion area was characterized by hypertrophic astrocytes with multiple $GFAP^+$ processes for both day 1 (**Figures 2d** and **2f**) and 28 (**Figures S1** and **S2**) post-injury, matching the appearance of SCI-associated local astrogliosis.[26] The GFAP immunoreactivity near the injury site was higher than that located further (> 10 mm) from the traumatic lesion area (**Figure 2h**). Specifically, we observed 29.4 ± 9.9% and 36.0 ± 17.8% GFAP intensity increase at 1 and 28 days post-injury, respectively, adjacent to the lesion area for SCI group. In the AcDX group, peritraumatic astrocytes were morphologically indistinguishable from astrocytes located distal to the injury site for both day 1 (**Figures 2e** and **g**) and 28 (**Figure S3** and **S4**) post-injury. At day 1 post-injury, the GFAP intensity of peritraumatic astrocytes was 15.0 ± 2.7% higher than that located further from the traumatic lesion area. This effect was continuous, because the peritraumatic GFAP intensity was only 8.1 ± 6.7% higher than that located further from the traumatic lesion area at day 28 post-injury. Hence, AcDX treatment significantly ($P < 0.05$, for both day 1 and 28 post-injury) and persistently inhibited the astrocytic response, as well as reduced the severity of initial reactive gliosis after SCI.

To evaluate the effect of AcDX treatment on microglial activation following SCI, we also quantified the number of activated microglial cells adjacent to the injury site and in the traumatic lesion area by immunodetection of $CD68^+$ microglia (**Figures 2d**, **2e**, **S1** and **S3**). At both day 1 and 28 post-injury, we did not observe any notable difference (**Figure S5**) on the number of $CD68^+$ cells in the peritraumatic area between the SCI only and AcDX groups. In contrast, a significant reduction in the number of $CD68^+$ microglia in the traumatic lesion area was observed with AcDX treatment compared to rats injected with only PBS at both day 1 ($P = 0.004$) and 28 ($P < 0.001$) post-injury (**Figure 2i**). In the lesion area, the density of microglia was 931 ± 75 per square millimeter at day 1 post-injury. After extending the time to 28 days after injury, the density of $CD68^+$ microglia increased to 2421 ± 234 per

square millimeter. Regarding the AcDX group, the $CD68^+$ microglia density only slightly increased from 727 ± 51 to 840 ± 219 per square millimeter within 28 days. At day 28 post-injury, a reduction in the number of $CD68^+$ microglia by about 65% in the traumatic lesion area was observed with AcDX treatment ($P < 0.001$) compared to rats injected with only PBS. Besides astrocytic response inhibition, AcDX efficiently restrained the inflammatory response associated to the microglia activation.[27]

Neurofilaments are cell type specific proteins in central nerve system, and qualified as potential surrogate markers of damage to neuron and axon.[28] The immunostaining analysis of 200 kDa subunit of neurofilament (NF200), which contributes to anomalous electrophoretic mobility, has been employed to evaluate the neuron and axon damage.[29] In the control (SCI) group (**Figures 2f** and **S2**), the NF200 immunoreactivity near the injury site was lower, 32.3 ± 1.7% and 29.8 ± 16.2% decrease at day 1 and 28 post-injury, than that located distant from the traumatic lesion area (**Figure 2**j). Regarding the AcDX group, the NF200 intensity of peritraumatic area was 19.2 ± 1.9% lower than that located further from the traumatic lesion area at day 1 post-injury (**Figures 2g** and **2j**). When the time extended to 28 days post-injury, the NF200 intensity of peritraumatic area was only 3.9 ± 5.5% lower than that located further from the traumatic lesion area for the AcDX group (**Figures S4** and **2j**). In comparison with the SCI only group, a significant increase ($P < 0.05$ for both 1 and 28 days post-injury) in NF200 labeling adjacent to the injury site was observed for AcDX treated group, suggesting the continuous neuronal protection effect of AcDX microspheres.

Western blot analysis was used to further validate the immunofluorescence analysis (**Figure 2k**). A semi-quantitative comparison of Western blot images showed that the GFAP expression in the AcDX group was significantly ($P = 0.048$) reduced as compared to the SCI only group (**Figure 2l**). Besides GFAP, the AcDX treatment also significantly ($P = 0.014$) reduced the CD68 expression (activation of microglia) at day 1 post-injury. A comparison of the NF200 expression demonstrated that AcDX treatment significantly ($P = 0.019$) protected neurons at day 1 post-injury. The Western blot analysis

results is highly consistent with the immunohistochemical studies, suggesting that AcDX can inhibit the reactivity of injury-related proteins and protect the injured neurons.

These immunohistochemistry results collectively demonstrate that AcDX microspheres not only suppressed the astrogliosis and inflammation, but also protected neurons, making AcDX a promising biomaterial for SCI treatment. The neuroprotective effect in the spinal cord tissue contributed to the rapid recovery of walking motion as early as 1 week after administration. The histological data corroborated the functional recovery results, showing that AcDX microspheres can enhance the recovery of injured spinal cord. However, the mechanism of neuronal protection by AcDX microsphere is unclear. In the following content, we further studied the possible mechanism for the attractive neuroprotection effect offered by AcDX microspheres.

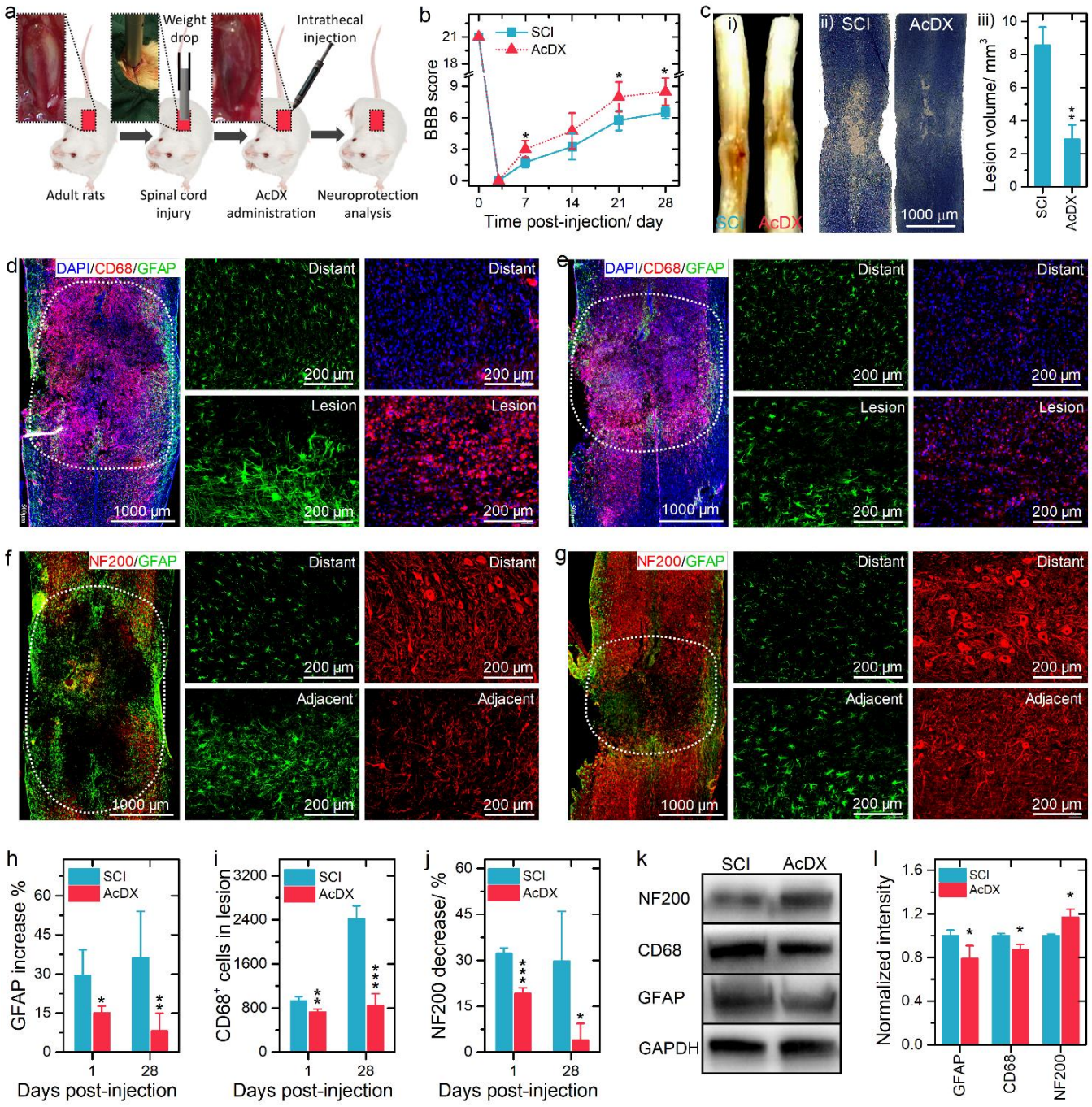

Figure 2. AcDX microspheres protect the traumatically injured spinal cord. (**a**) Schematic diagram of experimental design. AcDX microspheres were intrathecally injected within 5 min after weight drop at the T10 level. (**b**) The rats were functionally graded up to 28 days post-injury using the BBB grading scale (*n* = 5 animals per group). (**c**) Spinal cord at day 28 post-injury: (i) gross morphology, (ii) representative Nissl stained sagittal sections, and (iii) the lesion volumes (*n* = 3 animals per group). (**d** and **e**) Representative immunohistochemical staining images of GFAP (in green)

and CD68 (in red) in the spinal cord tissues of SCI (d) and AcDX (e) groups at day 1 post-injury. The boundary of cavity is indicated by the dashed lines. Right two columns are the enlarged images corresponding to the distant (> 10 mm) field to the lesion (upper row), and the lesion area (bottom row). The nuclei of all cells were stained with DAPI (in blue). (**f** and **g**) Representative immunohistochemical staining images of GFAP (in green) and NF200 (in red) in the injured spinal cord tissues of SCI (f) and AcDX (g) groups at day 1 post-injury. The dashed lines indicate the boundary of cavity. (**h-j**) Semi-quantification of GFAP intensity increase (h; $n \geq 5$ animals per group), the number of $CD68^+$ microglia in the traumatic lesion area (i; $n \geq 4$ animals per group), and NF200 intensity decrease (j; $n \geq 4$ animals per group). (**k**) Representative Western blots of NF200, CD68 and GFAP in lesion extracts at day 1 post-trauma. (**l**) Semi-quantification of relative expression level of NF200, CD68 and GFAP, normalized to GAPDH ($n = 3$ animals per group). Data present as mean ± s.d.; the levels of significance were set at probabilities of $^{*}P < 0.05$, $^{**}P < 0.01$, and $^{***}P < 0.001$.

Excitotoxicity is one of the most important pathological and neurochemical changes after SCI. Specifically, neurons are under the excessive stimulation by neurotransmitter GLU;[30] the high GLU concentration around the synaptic cleft induces the neuronal cell death. Neuron apoptosis contributes to the neuronal cell death and to the neurological dysfunction, induced by traumatic insults to the rat spinal cord.[31] We studied the neuronal apoptosis by propidium iodide (PI)/Hoechst 33342 (HC) staining (**Figure 3a**). The high intensity of PI indicates the cell death. HC staining was performed to visualize the nuclear morphology of neurons and to distinguish those apoptotic ones. The control neurons exhibited uniformly dispersed chromatin and intact cell membrane (PI-negative). The high magnification of neurons for each group is shown in **Figure S6**. After the administration of GLU, neurons exhibited typical characteristics of apoptosis, such as the condensation of chromatin, the shrinkage of nuclear, and the enhanced cell membrane permeability. We evaluated the neuroprotective

effect of AcDX microspheres on the GLU-induced excitotoxicity model. Three concentrations of AcDX microspheres, 0.25 mg/mL (AcDXL), 1.0 mg/mL (AcDXM) and 4.0 mg/mL (AcDXH), were selected for the following *in vitro* tests. Independent on the AcDX concentrations tested, the number of neurons with nuclear condensation and fragmentation decreased after AcDX microsphere treatment.

We further investigated the protection mode of AcDX microspheres by staining primary neurons with paired FITC-labelled annexin V (FAV; in green) and PI (in red), and then examined it by flow cytometry (**Figure 3b**). In terms of early apoptotic cells, there was a prolonged maintenance of membrane integrity and an externalization of phosphatidylserine to which the FAV could specifically bind. Live cells were negative for both stains, whereas early apoptotic cells were characterized by a high FAV signal in the absence of PI staining. The viability of neurons decreased to about 50% (**Figure 3c**) after GLU-induced excitotoxicity, about one third of neurons had lost membrane integrity (PI-positive; **Figure 3d**), and approximately 13% neurons were at the early apoptotic stage (FAV-positive and PI-negative; **Figure 3e**). Under the protection of AcDX microspheres, the viability of neurons was significantly improved ($P < 0.01$) for all three concentrations tested. As expected, the fraction of PI- and FAV-positive neurons significantly ($P < 0.01$) decreased when neurons were incubated with AcDX microspheres. The strongest protection effect was observed for the AcDXM group. The flow cytometry measurements were consistent with the fluorescence image analysis; both results indicated that AcDX microspheres can protect primary neurons from GLU-induced excitotoxicity.

Next, we analyzed the expression level of pro-apoptotic proteins (Calpain and Bax), anti-apoptotic protein (Bcl-2), and the apoptotic symbol caspases enzymes in primary neurons to preliminarily understand the mechanism of anti-apoptosis effect of AcDX microspheres (**Figure 3f**).[32] Among the caspases discovered, caspase-3 is an executioner of apoptosis, cleaving several essential downstream substrates.[33] Moreover, the activation of caspase-9, an important initiator of apoptosis, has been implicated in SCI.[34] The semi-quantitative analysis of Western blot images is presented in **Figure 3g**. Toward the GLU-induced excitotoxicity model, the significantly elevated expression level of Calpain

($P < 0.001$), Caspase-9 ($P = 0.011$) and Caspase-3 ($P = 0.003$), and Bax ($P = 0.004$) were observed in primary neurons, when compared to the PBS group. In contrast, the expression level of Bcl-2 notably decreased ($P < 0.001$) when GLU was added. After the administration of AcDX microspheres, the Western blot analyses revealed lower levels of Calpain and Caspase-9 and Caspase-3 than those of GLU group, whereas the expression of Bcl-2 improved. In terms of Bax, no significant difference was observed for the AcDXL and AcDXM groups when compared to the GLU group. The expression level of Bax for AcDXH was even significantly ($P = 0.002$) higher than that from the GLU group. The neuronal protection effect of AcDX microspheres can attributed to the attenuation of pro-apoptotic proteins (Calpain, Caspase-9 and Caspase-3) and the enhanced expression of anti-apoptotic protein (Bcl-2). Furthermore, the ratio of Bcl-2 to Bax is known as a key determinant of neuronal commitment to apoptosis.[35] Bcl-2/Bax increased for AcDX microspheres compared with GLU group, indicating that AcDX treatment inhibited the mitochondria-mediated cell death pathway.

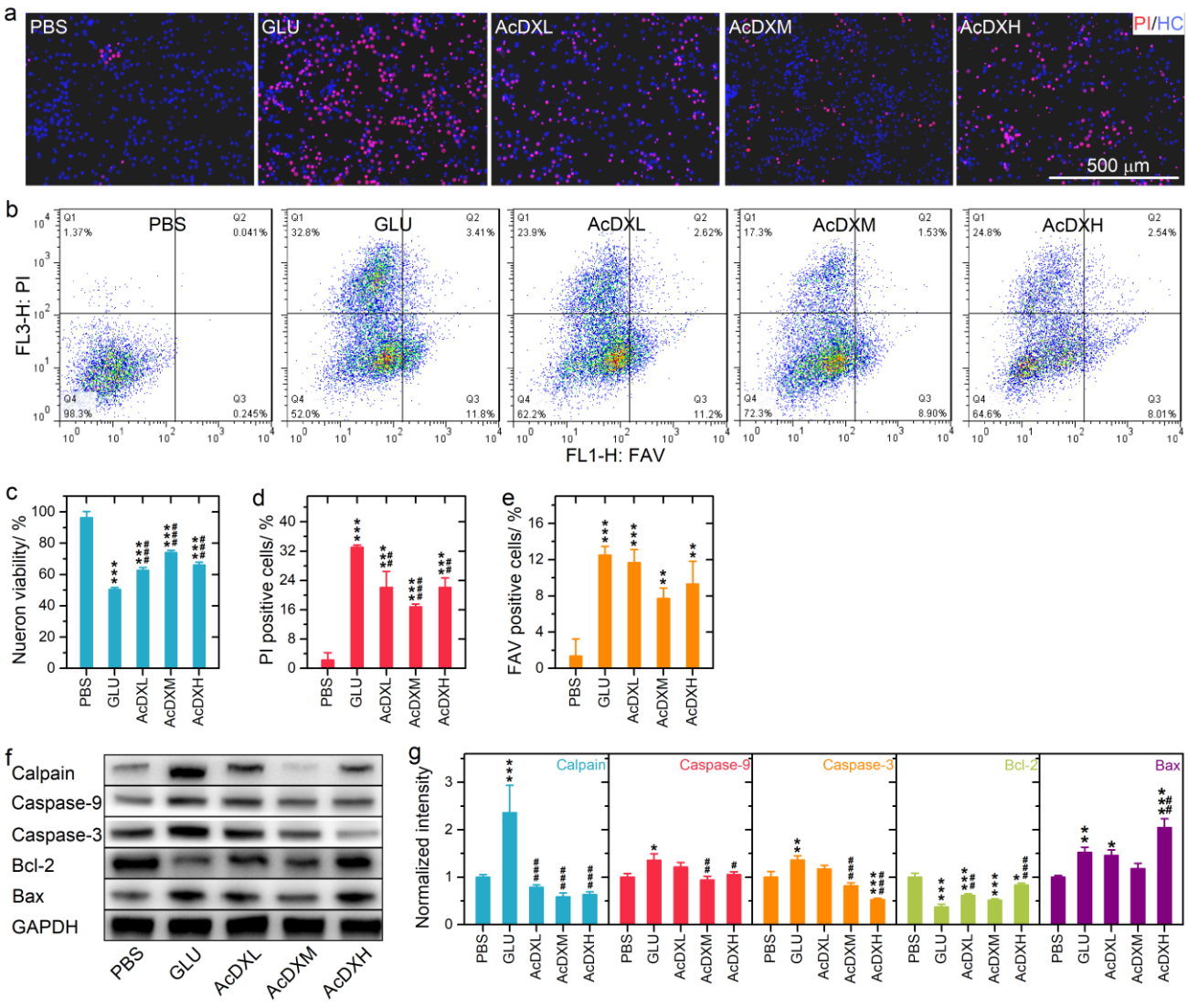

Figure 3. AcDX microspheres alleviate the GLU-induced neuronal apoptosis *in vitro*. For *in vitro* tests, the neurons were firstly incubated with microspheres for 15 min, followed by the administration of GLU (100 μM) for all the groups, except for the PBS one. (**a**) Representative fluorescence images of propidium iodide (PI, in red; marker of dead cells) and Hoechst 33342 (HC, in blue; nuclear marker for both survival and apoptotic cells) stained neurons incubated with AcDX microspheres after GLU-induced excitotoxicity. (**b**) Examples of scatter plots for neurons incubated with AcDX microspheres after GLU-induced excitotoxicity by PI/FAV double labeling. (**c**−**e**) Quantitative results of live (c), and PI- (d) and FAV-positive (e) neurons with and without the treatment by AcDX microspheres (*n* = 3). (**f**) Representative Western blot analysis of apoptosis indicated proteins in neurons incubated with AcDX microspheres after GLU-induced excitotoxicity. (**g**) Semi-quantification of relative expression

level of apoptosis indicated proteins in primary neurons, normalized to GAPDH (n = 3). The AcDX microspheres were compared with the groups of PBS (*) and GLU ($^{\#}$). Data present as mean ± s.d.; the levels of significance were set at probabilities of $^{*,\ \#}P < 0.05$, $^{**,\ \#\#}P < 0.01$, and $^{***,\ \#\#\#}P < 0.001$.

We assessed the extent of cell apoptosis in the peritraumatic zone of spinal cord by the terminal deoxynucleotidyl transferase-mediated dUTP nick end labeling (TUNEL) assay. The selected TUENL assay time point was 1 day post-injury, when a burst of neuronal and glial apoptosis in gray and white matter at the lesion site was observed.[31] The sagittal sections of the spinal cords treated with PBS and AcDX microspheres are presented in **Figure 4a**. High magnification of sagittal sections showed a clear cellular alteration of typical apoptosis, green colored and indicated by white arrows (**Figure S7**). On day 1 post-injury, the numbers of TUNEL-positive (apoptotic) cells for AcDX group was dramatically smaller (P = 0.006) than those treated with PBS (**Figure 4b**). The *in vivo* TUNEL assay confirmed that AcDX microspheres can effectively inhibit the cell apoptosis in the injured spinal cord, and these results are consistent with the *in vitro* tests.

The expression of apoptosis associated markers in the traumatic injured spinal cord was also evaluated by Western blot analysis (**Figure 4c**). The semi-quantitative comparison of Western blot images is shown in **Figure 4d**. The local delivery of AcDX microspheres prominently improved Bcl-2 (P = 0.022) expression and significantly reduced the expression level of Calpain (P < 0.001), Caspase-9 (P < 0.001), Caspase-3 (P = 0.012) and Bax (P = 0.002), as compared to the SCI only group. AcDX microspheres attenuated the pro-apoptotic proteins (Calpain, Caspase-9 and -3, and Bax) expression, and enhanced the expression of anti-apoptotic protein (Bcl-2), which corroborates the *in vitro* tests (**Figures 3f** and **3g**). In comparison to the SCI group, the higher Bcl-2/Bax ratio for the AcDX group indicates that the mitochondria-mediated cell death pathway in injured spinal cord can be blocked by AcDX spheres.

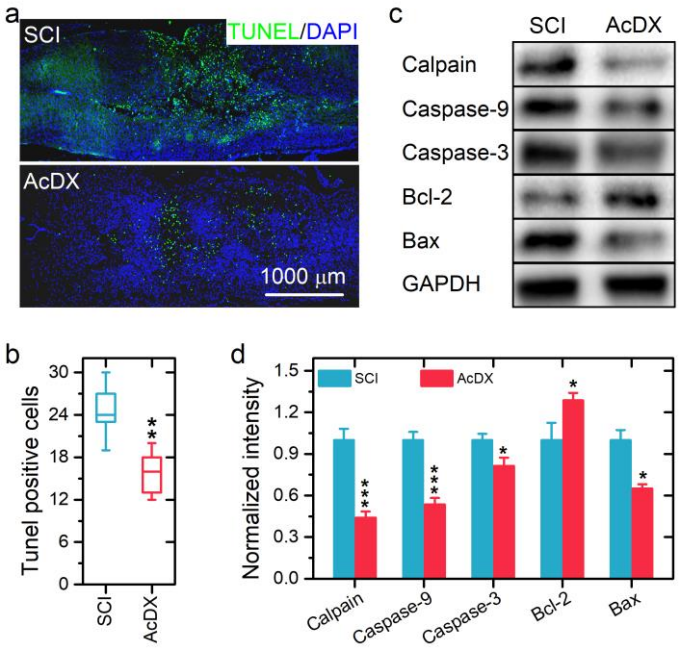

Figure 4. AcDX microspheres protect the injured neurons from apoptosis *in vivo*. (**a**) Representative images of TUNEL-positive apoptotic cells (in green) in sagittal spinal cord sections at day 1 post-trauma. The nuclei of all cells were stained with DAPI (in blue). (**b**) Comparison of the number of TUNEL-positive cells with and without AcDX microspheres treatment (n = 5 animals per group). (**c**) Representative Western blots of apoptosis indicated proteins in lesion extracts at day 1 post-trauma. (**d**) Semi-quantification of relative expression level of apoptosis indicated proteins, normalized to GAPDH. In terms of *in vivo* tests, the vehicle PBS served as the control (SCI group; n = 3 animals per group). Data present as mean ± s.d.; the levels of significance were set at probabilities of $^{*}P < 0.05$, $^{**}P < 0.01$, and $^{***}P < 0.01$.

In general, the pathologically high level of GLU can cause excitotoxicity by sustained calcium ion influx through GLU receptor channels, which is a common pathway of neuronal apoptosis.[36] We employed a calcium indicator, Fluo-4 AM ester, to monitor the intracellular calcium transients before and after the AcDX microsphere treatment.[37] Calcium influx by microscopy live imaging was determined over 5 min after establishing a baseline; F_0 is the baseline of Fluo-4 intensity and ΔF is the

change of Fluo-4 intensity in comparison to F_0. The time course of the Fluo-4 signals ($\Delta F/F_0$) as a function of time has been presented in **Figure 5a**. The GLU stimulation increased the peak intensity of Fluo-4 by approximately 5-fold, and peaked after approximately 2 min GLU stimulation. The incubation with ACDX microspheres before GLU stimulation effectively reduced the peak intensity of Fluo-4 for neurons. Specifically, the intracellular peak level of Fluo-4 reduced by approximately 30% (P = 0.041), 41% (P = 0.001) and 45% (P < 0.001) for AcDXL, AcDXM and AcDXH groups, respectively, in comparison with the GLU group (**Figure 5b**). After 5 min GLU stimulation, the Fluo-4 intensity difference was only observed between GLU and AcDXM (P = 0.019). **Figure 5c** shows the representative Fluo-4 fluorescence images of GLU-stimulated neurons incubated with different concentrations of AcDX microspheres. Overall, the neuronal protection effect of AcDX microspheres could be ascribed to the reduced calcium influx into neurons, which has also been observed for the poly(ethylene glycol)−poly(D,L-lactic acid) block copolymer.[7]

The high calcium ion loads increase the risk for mitochondrial damage, triggering the mitochondrial production of reactive oxygen species (ROS).[38] Hence, we monitored the intracellular ROS level to further corroborate the neuronal protection effect of AcDX microspheres.[39] The cell-permeant 2',7'-dichlorodihydrofluorescein diacetate (H_2DCFDA) was used as an indicator to detect the intracellular level of ROS in injured neurons. Oxidation of H_2DCFDA, forming highly fluorescent 2',7'-dichlorofluorescein (DCF), as determined using confocal microscopy was barely detectable in uninjured neurons (**Figure 5d**). The intensity of DCF fluorescence in GLU incubated neurons was markedly increased. Meanwhile, the administration of AcDX microspheres reduced the level of DCF fluorescence. The intensity changes of intracellular DCF fluorescence in different groups were confirmed by flow cytometry analysis (**Figures 5e** and **5f**). Based on the MFI values, only the intracellular ROS level for AcDXM group was notably (P < 0.05) lower than that of the GLU group.

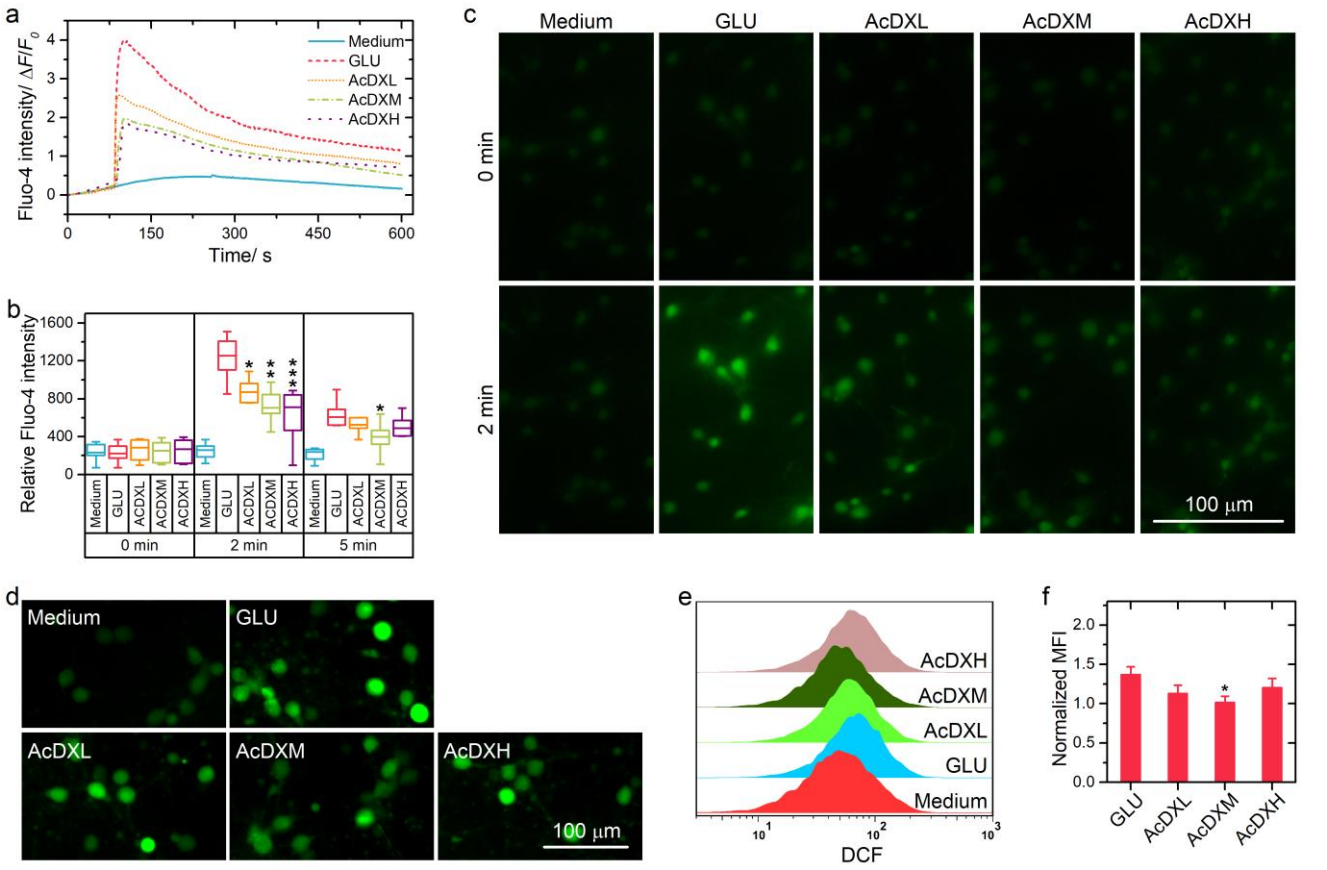

Figure 5. AcDX microspheres reduce the GLU-induced calcium ion influx and production of reactive oxygen species. (**a**) The time course of the Fluo-4 signals ($\Delta F/F_0$) as a function of time, with F_0 being the baseline Fluo-4 fluorescence and ΔF the change of Fluo-4 fluorescence in comparison to F_0. (**b**) Quantification of regions of interest demonstrating the effect of AcDX microspheres on reducing the fluorescence over time in response to GLU (n = 11). (**c**) Representative calcium images of neurons incubated with AcDX microspheres before (0 min) and after (2 min) GLU stimulation. (**d-f**) Representative ROS imaging (d), flow cytometry histograms (e), and the corresponding MFI (f; n = 3) of injured neurons incubated with AcDX microspheres. The MFI values were normalized to that of the PBS group. Data present as mean ± s.d.; the groups treated with AcDX microspheres were compared with the GLU group (*); the levels of significance were set at probabilities of $^{*}P < 0.05$, $^{**}P < 0.01$ and $^{***}P < 0.001$.

Lohmann *et al.*[40] synthesized glycosaminoglycan-based hydrogels, which can capture inflammatory chemokines to accelerate the wound healing. Inspiring by this inflammatory chemokine capture, we hypothesize that AcDX microspheres can alleviate the GLU-induced excitotoxicity through the physical adsorption of GLU. To verify this hypothesis, we evaluated the adsorption kinetics of GLU to AcDX microspheres, which was determined by incubation with 50 μM of GLU in artificial CSF (aCSF) As illustrated in **Figure 6a**, the more AcDX microsphere we added, the more GLU was adsorbed. For example, the adsorption of GLU up to about 6% was achieved, when the concentration of AcDX microspheres was 1 mg/mL. Moreover, the adsorption capacity of AcDXM and AcDXH for GLU was analyzed by incubating with a variety concentration of GLU in aCSF (25, 50 and 100 μM) for 30 min (**Figure 6b**). A linear correlation of the amounts of deployed and adsorbed GLU was found for both AcDXM and AcDXH. By increasing the GLU concentration from 25 to 100 μM, the percentage of GLU sequestered by AcDX microspheres decreased from 8% to 4% for AcDXM, and reduced from 22% to 10% for AcDXH.

We further verified the GLU capture capability of AcDX microspheres *in vivo* (**Figure 6c**). Detailed CSF sampling (100-150 μL) has been illustrated in **Video S1**. The GLU content in CSF was analyzed by an ultra-performance liquid chromatography and tandem mass spectrometry; a representative chromatogram of GLU in the CSF sample from the SCI only group at day 2 post-injury has been presented in **Figure S8**. Before injury, the GLU concentration in CSF is approximately 4 μM (t = day 0). For both SCI and AcDX groups, the GLU concentration in CSF continually increased until day 2 post-injury, and then decreased to a level (approximately 2 and 1 μM for SCI and AcDX, respectively) even lower than the normal GLU concentration (4 μM). Until day 4 post-injury, the GLU concentration for AcDX group was always significantly lower than that for the SCI only group. Specifically, after the administration of AcDX microspheres, the GLU concentration decreased from approximately 18 to 8 μM ($P < 0.05$) at 8 h post-injury, from approximately 77 to 58 μM ($P < 0.001$) at day 2 post-injury, and from approximately 64 to 53 μM ($P < 0.001$) at day 4 post-injury. We also calculated the area

under the curve (AUC) of GLU concentrations in CSF (**d**). The AUC of GLU for the group treated by AcDX microspheres was also significantly ($P < 0.01$) lower than that of the SCI only group. Based on both *in vitro* and *in vivo* GLU adsorption results, we can conclude that our AcDX microspheres can protect neurons from excitotoxicity by sequestering the GLU in CSF.

The overload of calcium ions is one of the most important features for the GLU-induced excitotoxicity, hence we also evaluated the adsorption capability of AcDX microspheres toward calcium ions. Surprisingly, the AcDX microspheres can also scavenge the calcium ions in aCSF (**Figure 6e**). This calcium ion scavenging capability of AcDXM and AcDXH was also confirmed by the relation between the deployed and adsorbed calcium ions (**Figure 6f**). Like the sequestering effect toward GLU in CSF, the administrated AcDX microspheres also reduced the intensity of the calcium ions in CSF (**Figure 6g**). In comparison to the SCI group, significantly lower calcium ion concentrations were observed at 8 h ($P < 0.05$), and day 1 ($P < 0.01$), 2 ($P < 0.001$) and 4 ($P < 0.001$) post-injury; the AUC of calcium ions for the group treated by AcDX microspheres was also significantly reduced ($P < 0.001$; **Figure 6h**). Therefore, the neuronal protection effect of AcDX microspheres can also be partially ascribed to their calcium ion scavenging feature.

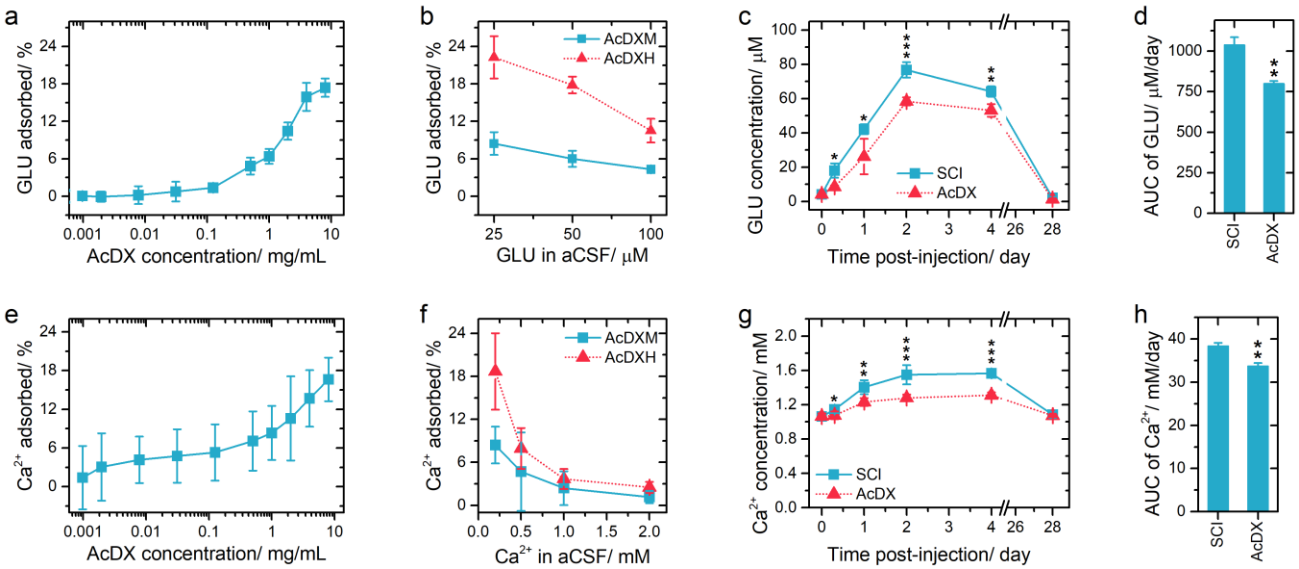

Figure 6. AcDX microspheres alleviate GLU-induced excitotoxicity by sequestering GLU and calcium ions. (**a**) The adsorption of GLU (50 μM) by AcDX microspheres in aCSF in terms of the microsphere concentrations (n = 6). (**b**) The impact of GLU concentrations on the adsorption of GLU by AcDX microspheres in aCSF (n = 6). (**c** and **d**) The effect of AcDX microspheres on the concentrations of GLU in the CSF as a function of time (c; $n \geq 3$ animals per time point) and the corresponding area under curve (d; n = 3). (**e**) The adsorption of calcium ions (0.5 mM) by AcDX microspheres in aCSF in terms of the microsphere concentrations (n = 6). (**f**) The impact of calcium ion concentrations on the adsorption of calcium ions by AcDX microspheres in aCSF (n = 6). (**g** and **h**) The effect of AcDX microspheres on the concentrations of calcium ions in the CSF as a function of time (g; $n \geq 3$ animals per time point) and the corresponding area under curve (h; n = 3). Data present as mean ± s.d.; the groups treated with AcDX microspheres were compared with the SCI only group (*); the levels of significance were set at probabilities of $^{*}P < 0.05$, $^{**}P < 0.01$ and $^{***}P < 0.001$.

GLU and calcium ions play a key role in excitotoxicity, which leads to neuronal cell apoptosis.[41] AcDX microspheres show the capability of buffering out excess GLU and calcium ions. Benefiting from the fast sequestering of GLU and calcium ions by AcDX microsphere, significantly lower level of GLU and calcium ions in CSF has been achieved at the first evaluation time point (8 h post-injury). By reducing the magnitude of the initial increase of extracellular GLU and calcium ions during the acute (2-48 h post-injury) and subacute (2-14 days post-injury) phases of SCI,[42] AcDX microspheres successfully attenuate the degree of excitotoxic secondary neuron damage. Like FITC-dextran and FITC (**Figure 1f**), the sequestered GLU and calcium ions will be released into CSF during the AcDX degradation process. Based on the degradation rate of AcDX microspheres, GLU and calcium ions being released from microspheres is unlikely to be cytotoxic, especially at the acute and subacute phases of SCI. During the chronic phase of SCI, the cellular mitochondrial storage, and astrocytic

connections to the vascular system through the blood brain barrier would work to prevent the reestablishment of cytotoxic level of GLU and calcium ions.[43] Our finding implies that AcDX microspheres should be administrated as soon as possible following the initial injury to maximize their therapeutic efficacy. These results provide an interesting potential drug delivery application for our microspheres during the acute/subacute phase of SCI.

This study demonstrates that the intrathecal administration of bare AcDX microspheres can protect neurons from GLU-induced excitotoxicity, and therefore, repair the injured spinal cord. The neuroprotective feature of AcDX microspheres is achieved by sequestering GLU and calcium ions in CSF, reducing the calcium ions influx into neurons and inhibiting the formation of ROS. Consequently, AcDX microspheres attenuate the expression of pro-apoptotic proteins (Calpain and Bax) and enhance the expression of anti-apoptotic protein (Bcl-2) both *in vitro* and *in vivo*. The intrathecal administration of AcDX microspheres immediately after traumatic injury leads to histological protection in spinal tissue and functional recovery in live animals. The administration of such microspheres or scaffolds may play an important role in the design of future strategies for the treatment of traumatic central nervous system injury, not limited to SCI. For example, benefiting from the protection effect of AcDX, the incorporation of therapeutic compounds into the AcDX-based drug delivery systems and scaffolds may bring synergistic outcome toward the SCI therapy and the treatment of other traumatic central nervous system injury. Follow-up studies will aim to load therapeutics into the AcDX microspheres to further improve the recovery of the injured spinal cord. In summary, our work opens an exciting perspective toward the application of neuroprotective AcDX for the treatment of severe neurological diseases.

Supporting Information

Experimental section and supporting figures are enclosed in Supporting Information, which is available from the Wiley Online Library or from the authors.

Acknowledgements

D. Liu, J. Chen and T. Jiang contributed equally to this work. We acknowledge financial support from the Academy of Finland (Grant Nos. 308742, 252215 and 281300), Jane and Aatos Erkko Foundation (No. 4704010), Research Funds of the University of Helsinki, the European Research Council under the European Union's Seventh Framework Programme (FP/2007-2013, No. 310892), the National Natural Science Foundation of China (Grant Nos. 81772352, 81401807, 81772351 and 81271988), and Natural Science Foundation of Jiangsu Province (Grant No. BK2012876).

Received: ((will be filled in by the editorial staff))

Revised: ((will be filled in by the editorial staff))

Published online: ((will be filled in by the editorial staff))

Table of Contents

Intrathecally administrated acetalated dextran microspheres scavenge the glutamate and calcium ions in cerebrospinal fluid, attenuate the glutamate-induced excitotoxicity, and ultimately protect the injured spinal cord neurons in rats.

Keyword: spinal cord injury, acetalated dextran, neuroprotection, functional recovery, anti-apoptosis

Dongfei Liu, Jian Chen, Tao Jiang, Wei Li, Yao Huang, Xiyi Lu, Zehua Liu, Weixia Zhang, Zheng Zhou, Qirui Ding, Hélder A. Santos*, Guoyong Yin*, Jin Fan*

Biodegradable Spheres Protect Traumatically Injured Spinal Cord by Alleviating the Glutamate-Induced Excitotoxicity

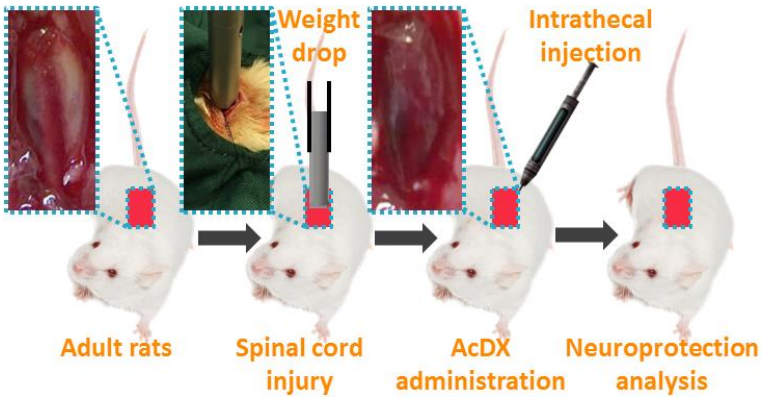

References:

[1] A. E. M. Mautes, M. R. Weinzierl, F. Donovan, L. J. Noble, Phys. Ther. 2000, 80, 673.

[2] a) S. B. Jazayeri, S. Beygi, F. Shokraneh, E. M. Hagen, V. Rahimi-Movaghar, Eur. Spine J. 2015, 24, 905; b) S. Thuret, L. D. Moon, F. H. Gage, Nat. Rev. Neurosci. 2006, 7, 628.

[3] D. D. French, R. R. Campbell, S. Sabharwal, A. L. Nelson, P. A. Palacios, D. Gavin-Dreschnack, J. Spinal Cord Med. 2007, 30, 477.

[4] A. K. Varma, A. Das, G. Wallace, J. Barry, A. A. Vertegel, S. K. Ray, N. L. Banik, Neurochem. Res. 2013, 38, 895.

[5] S. Kabu, Y. Gao, B. K. Kwon, V. Labhasetwar, J. Control. Release 2015, 219, 141.

[6] a) H. F. Wu, J. S. Cen, Q. Zhong, L. M. Chen, J. Wang, D. Y. B. Deng, Y. Wan, Biomaterials 2013, 34, 1686; b) D. Liu, T. Jiang, W. Cai, J. Chen, H. Zhang, S. Hietala, H. l. A. Santos, G. Yin, J. Fan, Adv. Healthc. Mater. 2016, 5, 1513.

[7] Y. Z. Shi, S. Kim, T. B. Huff, R. B. Borgens, K. Park, R. Y. Shi, J. X. Cheng, Nat. Nanotechnol. 2010, 5, 80.

[8] W. Wu, S. Y. Lee, X. Wu, J. Y. Tyler, H. Wang, Z. Ouyang, K. Park, X. M. Xu, J. X. Cheng, Biomaterials 2014, 35, 2355.

[9] a) G. C. de Ruiter, R. J. Spinner, M. J. A. Malessy, M. J. Moore, E. J. Sorenson, B. L. Currier, M. J. Yaszemski, A. J. Windebank, Neurosurgery 2008, 63, 144; b) J. R. Slotkin, C. D. Pritchard, B. Luque, J. Ye, R. T. Layer, M. S. Lawrence, T. M. O'Shea, R. R. Roy, H. Zhong, I. Vollenweider, V. R. Edgerton, G. Courtine, E. J. Woodard, R. Langer, Biomaterials 2017, 123, 63.

[10] S. F. Wang, D. H. Kempen, N. X. Simha, J. L. Lewis, A. J. Windebank, M. J. Yaszemski, L. C. Lu, Biomacromolecules 2008, 9, 1229.

[11] B. K. K. Chen, A. M. Knight, N. N. Madigan, L. Gross, M. Dadsetan, J. J. Nesbitt, G. E. Rooney, B. L. Currier, M. J. Yaszemski, R. J. Spinner, A. J. Windebank, Biomaterials 2011, 32, 8077.

[12] W. T. Daly, A. M. Knight, H. Wang, R. de Boer, G. Giusti, M. Dadsetan, R. J. Spinner, M. J. Yaszemski, A. J. Windebank, Biomaterials 2013, 34, 8630.

[13] E. M. Bachelder, T. T. Beaudette, K. E. Broaders, J. Dashe, J. M. Frechet, J. Am. Chem. Soc. 2008, 130, 10494.

[14] K. E. Broaders, J. A. Cohen, T. T. Beaudette, E. M. Bachelder, J. M. Frechet, Proc. Natl. Acad. Sci. USA 2009, 106, 5497.

[15] a) S. L. Suarez, A. Munoz, A. C. Mitchell, R. L. Braden, C. L. Luo, J. R. Cochran, A. Almutairi, K. L. Christman, ACS Biomater. Sci. Eng. 2016, 2, 197; b) S. Suarez, G. N. Grover, R. L. Braden, K. L. Christman, A. Amutairi, Biomacromolecules 2013, 14, 3927.

[16] J. W. McDonald, C. Sadowsky, Lancet 2002, 359, 417.

[17] S. Y. Teh, R. Lin, L. H. Hung, A. P. Lee, Lab Chip 2008, 8, 198.

[18] a) W. Li, D. Liu, H. Zhang, A. Correia, E. M. Mäkilä, J. Salonen, J. T. Hirvonen, H. A. Santos, Acta Biomater. 2017, 48, 238; b) D. Liu, H. Zhang, B. r. Herranz-Blanco, E. M. Mäkilä, V.-P. Lehto, J. Salonen, J. T. Hirvonen, H. l. A. Santos, Small 2014, 10, 2029; c) D. Liu, B. Herranz-Blanco, E. M. Mäkilä, L. R. Arriaga, S. Mirza, D. A. Weitz, N. Sandler, J. Salonen, J. T. Hirvonen, H. A. Santos, ACS Appl. Mater. Inter. 2013, 5, 12127.

[19] R. Vasiliauskas, D. Liu, S. Cito, H. Zhang, M. A. Shahbazi, T. Sikanen, L. Mazutis, H. A. Santos, ACS Appl. Mater. Inter. 2015, 7, 14822.

[20] Y. L. Lai, P. M. Smith, W. J. Lamm, J. Hildebrandt, J. Appl. Physiol. Respir. Environ. Exerc. Physiol. 1983, 54, 1754.

[21] P. R. Wich, J. M. J. Frechet, Aust. J. Chem. 2012, 65, 15.

[22] R. Di Terlizzi, S. Platt, Vet. J. 2006, 172, 422.

[23] J. C. Bresnahan, M. S. Beattie, F. D. Todd, D. H. Noyes, Exp. Neurol. 1987, 95, 548.

[24] M. T. Fitch, J. Silver, Exp. Neurol. 2008, 209, 294.

[25] J. C. Fleming, M. D. Norenberg, D. A. Ramsay, G. A. Dekaban, A. E. Marcillo, A. D. Saenz, M. Pasquale-Styles, W. D. Dietrich, L. C. Weaver, Brain 2006, 129, 3249.

[26] M. E. Schwab, Science 2002, 295, 1029.

[27] S. Papa, I. Caron, E. Erba, N. Panini, M. De Paola, A. Mariani, C. Colombo, R. Ferrari, D. Pozzer, E. R. Zanier, F. Pischiutta, J. Lucchetti, A. Bassi, G. Valentini, G. Simonutti, F. Rossi, D. Moscatelli, G. Forloni, P. Veglianese, Biomaterials 2016, 75, 13.

[28] A. Petzold, J. Neurol. Sci. 2005, 233, 183.

[29] R. Posmantur, R. L. Hayes, C. E. Dixon, W. C. Taft, J. Neurotrauma 1994, 11, 533.

[30] O. N. Hausmann, Spinal Cord 2003, 41, 369.

[31] X. Z. Liu, X. M. Xu, R. Hu, C. Du, S. X. Zhang, J. W. McDonald, H. X. Dong, Y. J. Wu, G. S. Fan, M. F. Jacquin, C. Y. Hsu, D. W. Choi, J. Neurosci. 1997, 17, 5395.

[32] D. W. Nicholson, N. A. Thornberry, Trends Biochem. Sci. 1997, 22, 299.

[33] J. E. Springer, R. D. Azbill, P. E. Knapp, Nat. Med. 1999, 5, 943.

[34] S. Krajewski, M. Krajewska, L. M. Ellerby, K. Welsh, Z. Xie, Q. L. Deveraux, G. S. Salvesen, D. E. Bredesen, R. E. Rosenthal, G. Fiskum, J. C. Reed, Proc. Natl. Acad. Sci. USA 1999, 96, 5752.

[35] J. Qiu, O. Nesic, Z. Ye, H. Rea, K. N. Westlund, G. Y. Xu, D. McAdoo, C. E. Hulsebosch, J. R. Perez-Polo, J. Neurotrauma 2001, 18, 1267.

[36] a) X. X. Dong, Y. Wang, Z. H. Qin, Acta Pharmacol. Sin. 2009, 30, 379; b) M. Ankarcrona, J. M. Dypbukt, E. Bonfoco, B. Zhivotovsky, S. Orrenius, S. A. Lipton, P. Nicotera, Neuron 1995, 15, 961; c) J. F. Stover, A. W. Unterberg, Brain Res. 2000, 875, 51.

[37] a) C. Grienberger, A. Konnerth, Neuron 2012, 73, 862; b) M. M. Harraz, S. M. Eacker, X. Q. Wang, T. M. Dawson, V. L. Dawson, Proc. Natl. Acad. Sci. USA 2012, 109, 18962.

[38] A. Atlante, P. Calissano, A. Bobba, S. Giannattasio, E. Marra, S. Passarella, FEBS Lett. 2001, 497, 1.

[39] A. C. Rego, C. R. Oliveira, Neurochem. Res. 2003, 28, 1563.

[40] N. Lohmann, L. Schirmer, P. Atallah, E. Wandel, R. A. Ferrer, C. Werner, J. C. Simon, S. Franz, U. Freudenberg, Sci. Transl. Med. 2017, 9.

[41] C. A. Oyinbo, Acta Neurobiol. Exp. 2011, 71, 281.

[42] R. G. Grossman, R. F. Frankowski, K. D. Burau, E. G. Toups, J. W. Crommett, M. M. Johnson, M. G. Fehlings, C. H. Tator, C. I. Shaffrey, S. J. Harkema, J. E. Hodes, B. Aarabi, M. K. Rosner, J. D. Guest, J. S. Harrop, J. Neurosurg. Spine 2012, 17, 119.

[43] a) D. K. Anderson, L. D. Prockop, E. D. Means, L. E. Hartley, J. Neurosurg. 1976, 44, 715; b) N. J. Olby, N. J. H. Sharp, K. R. Munana, M. G. Papich, J. Neurotrauma 1999, 16, 1215.

Video of CSF Sample Collection

Click here to access/download
Supporting Information
video of CSF Sample Collection.mp4

Figure 1

Click here to access/download

Production Data

Figure 1.tif

Figure 2

Figure 3

Click here to access/download

Production Data

Figure 3.tif

Figure 4

Figure 5

Figure 6